GOING THE DISTANCE:

INCREASING AERODYNAMIC EFFICIENCY IN ELECTRIC MOTORCYCLES WITH THE ADDITION OF A REAR FAIRING

by

NOAH MIFSUD

A THESIS

Presented to the Department of Physics
and the Robert D. Clark Honors College
in partial fulfillment of the requirements for the degree of
Bachelor of Science

June 2020

An Abstract of the Thesis of

Noah Mifsud for the degree of Bachelor of Science
in the Department of Physics to be taken June 2020

Title: Going the Distance: Increasing Aerodynamic Efficiency in Electric Motorcycles Through the Addition of a Rear Fairing

Approved: ___*Ben McMorran, Ph.D.*_____
Primary Thesis Advisor

With the current industry shift to electrification, one of the largest hurdles manufacturers face in motivating widespread adoption of battery electric vehicles is achieving extended range. The longest-range electric motorcycles on the market today can cover just over 160 km during freeway cruising. Low aerodynamic efficiency, resulting from turbulent, low pressure areas created behind the rider's torso and legs, is a significant contributor to this limited freeway range. This thesis describes the process of designing and testing an extended rear fairing which works in conjunction with the front fairing to create steady laminar flow passing over the rider and continuing along a gently tucking tail section to increase aerodynamic efficiency.

This thesis begins by outlining the current state of motorcycle design and providing background on aerodynamics and computational fluid dynamics (CFD). It then describes the process of constructing a digital model of the proposed design in computer aided design (CAD) software and testing it using CFD simulations. Results of these simulations are then analyzed focusing on the reduction in drag coefficient and on stability in cross wind scenarios. It finds that the drag coefficient of a motorcycle can be

reduced by up to 0.06 through the addition of a rear fairing positioned behind the rider and partially covering the rear wheel. Additionally, this rear fairing reduces aerodynamic lift by 50% and, in crosswind scenarios, reduces the yaw torque by 7.5% but increases the roll torque by 23%.

Acknowledgements

I owe my gratitude to my advisor, Professor Ben McMorran, for listening to my ideas and supporting me through each step of this process. From initial planning to serving on my thesis committee, he has been there. I would like to thank Dr. Barbara Mossberg for supporting my many endeavors, this thesis included, and for serving on my thesis committee. I would also like to thank Rich Moraski for serving as member of my committee and bringing his skill and perspective to my project.

I must express my sincerest gratitude to the Clark Honors College for the opportunity to undertake this project, as well as providing me with the support and necessary skills to create something cool.

Finally, I would like to thank my whole family for supporting me throughout this process and listening to me talk endlessly about my project, you have been the best.

For Finn.

Table of Contents

Introduction 1

A Model for Predicting Range 5

The Task 7

Motorcycle Aerodynamics 10

Principles of Aerodynamics 11

Aerodynamic Stability 16

My Concept Rear Fairing Design 22

Computational Fluid Dynamics 24

CFD Theory 26

Practical Implementation 29

How to Interpret CFD Images 31

Models, Methods and Experimental Setup 33

Making a Motorcycle 34

Making a Virtual Wind Tunnel 42

Results 47

Phase One: Establishing Consistency 48

Phase Two: Relationship Between Front Fairing Cd and Rear Fairing Performance 53

Phase Three: Cross Wind Scenarios and Porous Fairings 56

Discussion of Results 61

Conclusion 63

Appendix: Additional Figures and Tables 65

Bibliography 67

List of Figures

Figure E.1: Equation for Range in Terms of Drag Coefficient and Frontal Area. 6

Figure 0.1: Graph of Drag Coefficient vs Range for Zero SR like Motorcycles. 6

Figure 1.1: Depiction of Flows Around Various Objects. 13

Figure E.2: Equation for Force in Terms of Drag Coefficient and Frontal Area. 14

Figure 1.2: Simple Illustration of the Problem with Front-Fairinged Motorcycle Design. 15

Figure E.3: Equation Relating Torque to Force Magnitude and Distance of Application from Axis of Rotation or Center of Mass. 18

Figure 1.3: Forces Being Applied a Distance *r* From the Center of Mass 19

Figure 1.4: Overview of My Concept Rear Fairing Design 22

Figure 2.1: Solid Section of a CAD Model After Being Subdivided into Discrete Cells. 27

Figure 2.2: Particle Path Trace of the Flow Over a Motorcycle. 31

Figure 3.1: Exploded View of Standard Motorcycle 35

Figure 3.2: Models F2, SF, FH and SFH 38

Figure 3.3: NF1 vs NF2 40

Figure 3.4: Changes Made During the Redesign of the Rear Fairing 41

Figure 3.5: F2 vs SF 42

Figure 3.6: Wind Tunnel Design 43

Figure 3.7: Wind Tunnel Adapted to Crosswind Scenario 44

Figure 4.1: Graph NF1 vs F1 51

Figure 4.2: Flow Around NF1 vs F1 52

Figure 4.3: Graph Comparing NF1, F1, NF2 and N2F1 55

Figure 4.4: Flow Around F2 57

Figure 4.5: Comparison Graph of the Measured Drag Coefficients of NF2, F2, SF, FH and SFH 58

Figure 4.6: Comparison of the Center of Horizontal Force Between NF2 and F2 60

Figure A.1: The Anatomy of a Motorcycle 65

Figure A.2: Values Used in the Range Estimation Equation 65

Figure A.3: Vortex Formation Around the Edge of an Object in a 2-dimensional CFD Simulation. 65

List of Tables

Table 1: NF1 Results 48

Table 2: F1 Results 50

Table 3: Performance Comparison of NF1-F1 and NF2-N2F1 54

Table 4: F2 Results 56

Table 5: Crosswind Test Results Comparison for NF2, F2, SF, FH and SFH 59

Table A.1: NF2 Results 66

Table A.1: N2F1 Results 66

Table A.3: SF Results 66

Table A.4: FH Results 66

Table A.5: SFH Results 66

Introduction

Vehicle ownership is a cornerstone of American Culture. For some people, these vehicles are merely a necessity, a means to get from point A to point B in our sprawling, car-centric cities or across vast distances within and between States or countries. For others, cars, motorcycles, and vehicles of all sorts are objects of passion. We lovers of speed, power and handling often feel as if the desire to drive and ride is embedded in our very DNA. Regardless of the motivation for owning them, in face of the scientifically proven reality of climate change, it is undeniable that use of vehicles is directly contributing to rendering our planet unlivable.

Transportation accounted for 28% of all energy consumed and 29% of all greenhouse gas emissions in the United States in 2018.[5][16] From the materials and labor used during manufacturing, to the fuels burned for power, to the eventual dismantling and decay whilst rotting in a junkyard, vehicles are pervasive pollutants. Yet they persist as a source of pleasure as well as necessity in our society. The ability to quickly move from place to place, travelling distances both long and short, is a requisite that cannot be ignored; we can’t simply walk or bike from Eugene to Portland (a distance some 120 miles) because it’s best for our environment. To preserve our freedom to travel, and the passion for vehicles, we must continue striving to develop methods and adaptations that allow us to sustainably roam the planet without destroying it.

One of the most promising potential options for making our transportation more environmentally friendly is electrification. Provided there is a way to store and transform it into motion, electricity can be easily generated from renewable resources.

As long as renewable energy continues to develop, electric vehicles will be powered completely sustainably. However, electric vehicles still face a major hurdle to replacing their gas-powered counterparts: range.

We’re accustomed to modes of transportation that allow us to travel three-hundred or four-hundred miles on a single tank of gas. A tank that can be effortlessly replenished in a matter of minutes at one of countless petrol stations along every route. Comparably, the ranges and charging infrastructures of electric vehicles are, at present, quite limited. At the end of the day, consumers seeking to invest in a mode of transportation are more likely to purchase the vehicle best suited to their needs, ideally one that proves efficient and convenient to their lifestyle. If we want to motivate adoption of electric vehicles on a mass scale, they must ultimately be capable of performing as well, if not better than, what they are replacing.

Pending a quantum leap in battery technology, electric vehicles will be somewhat hindered by the storage capacity and weight of batteries. Batteries are essentially dense lumps of metal and battery powered vehicles are customarily heavier than their gasoline counterparts. In lieu of adding more batteries and more weight to increase range, it is best to ensure every single drop of power is transmitted to motion, not wasted in inefficiencies.

In an attempt to approach this issue and explore possible areas of improvement, I homed in on the development of electric motorcycles. The motorcycle market has been slower to shift to electric power than the automotive market, due predominantly to this issue of weight. A motorcycle must be balanced by its rider at low speeds and kept upright during high speed turns. Add too much weight, and this becomes challenging

and unpleasant. As a result, electric motorcycles suffer from poor ranges, significantly lower than those of their gasoline counterparts. The longest-range electric motorcycles on the market today can cover a maximum 160 km (100 miles) during freeway cruising which severely limits their usability beyond city commuting.[19] This makes convincing people that electric motorcycles are an optimal mode of transportation difficult. Riders would likely need to recharge while making the simple, short trip from Eugene to Portland. Recognizing this, I searched for ways to improve motorcycle efficiency by design.

Since motorcycles are essentially the least amount of metal and structure which can enable a rider to attach themselves to an engine and steer, they are already fairly light and relatively minimalist machines, so improvements from weight reduction or increased drivetrain efficiency are unlikely. However, it turns out that motorcycles are severely aerodynamically inefficient.[8][13][15] There is an absolute measurement called drag coefficient (Cd) used to determine the aerodynamic efficiency of a shape, regardless of its size. The average passenger car will have a Cd value around 0.2 or 0.3 while a large truck might approach 0.5[1]. The most aerodynamically efficient motorcycles right now have a Cd value of around 0.4. An average motorcycle would be much closer to 0.7.[8] For freeway cruising, this becomes particularly detrimental to range.

It is accepted the amount of force required to move a vehicle through air will increase relative to the square of its speed. Double the speed and the force of air will

[1] Lower Numbers are more efficient

quadruple. This means that at freeway speeds, a motorcycle will expend most of its energy overcoming aerodynamic force.

The challenge faced in attempting to design an aerodynamically efficient motorcycle is overcoming the negative effects of the rider.[15] The rider's body disrupts the low drag flow of air passing over smooth surfaces or traveling uninterrupted and creates turbulence. This, coupled with the empty space behind the rider and in the rear section of a motorcycle, creates a vacuum like effect, sucking the entire rider+bike system backwards. Up until the development of electric motorcycles, designers have not had to worry about these poor aerodynamic properties. Motorcycles are light, and gasoline powered motorcycle engines are already efficient and power dense. Designers have been able to guilelessly add power to their engines to override aerodynamic drag, while still creating vehicles that return impressive fuel economy numbers.[8]

To increase the efficiency of motorcycles, particularly electric motorcycles, and in the effort to improve their competitiveness and increase adoption, I devised a method for reducing aerodynamic drag.

Modern sports and sport-touring motorcycles use devices called fairings to improve their aerodynamic efficiency. A fairing is a piece of shaped material, usually plastic or carbon-fiber, whose main purpose is to affect the aerodynamics of a vehicle. When picturing a race motorcycle, the smooth, swoopy colored piece of plastic on the front, giving these bikes their distinctive shape, is the fairing[2]. The current crop of electric motorcycles features mostly 'naked' bikes with no fairings or windshields at all.

[2] For an overview of the anatomy of a motorcycle, see Figure A.1 in the Appendix.

While this design is sometimes considered more stylish, it is not aerodynamically efficient. Adding classical front fairings, as commonly seen on sports/super bikes would reduce drag, however, these fairings have only been designed to manage airflow over the front half of the bike. To mitigate the negative effects of turbulence and low-pressure areas behind the rider I designed an extended rear fairing.

This rear fairing is meant to work in conjunction with the front fairings to create steady, smooth airflow passing over the rider and continuing behind along a gently tucking tail section. While no reasonable bodywork could eliminate the turbulence and vacuum effects of the rider's torso, my proposed fairing should vastly reduce those negative effects from the waist down and across the rear section of the bike, resulting in increased aerodynamic efficiency and extended freeway range.

A Model for Predicting Range

Design and incorporation into production of a refined rear fairing could significantly increase the freeway range of modern electric motorcycles and motivate their adoption. The most popular electric motorcycle on sale at the time of writing is the Zero SR, a naked bike which has a freeway range of only 102 miles (163 kilometers) [19]. To illustrate how significant an effect a lowered drag coefficient could have on freeway range, I created Figure 0.1. Using the SR's weight and battery capacity as an example, while assuming a constant speed of 112.7 km/h (70 mph) though unperturbed air on flat ground at sea level[3], I plotted Equation 1 (Figure E.1) for range in terms of drag coefficient and frontal area.[6][12]

[3] See Figure A.2 in the Appendix for list of assumed values.

$$r = \frac{3600 * E}{mgf + 0.0386(\rho * C_x A v^2)}$$

Figure E.1: Equation for Range in Terms of Drag Coefficient and Frontal Area.

E is the total energy capacity of the motorcycle, *m* its mass, *g* acceleration due to gravity, *f* a measure of friction in the tires, *ρ* the density of air, C_x drag coefficient, *A* frontal area, and *V* velocity.

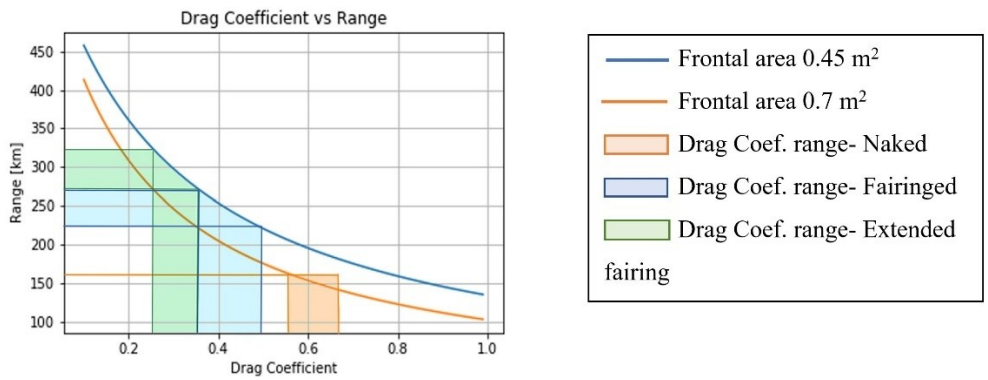

Figure 0.1: Graph of Drag Coefficient vs Range for Zero SR like Motorcycles.

The lower curve uses the average frontal area of a naked bike of 0.7m^2 while the upper curve uses the average for fairinged bikes, 0.45m^2. The orange horizontal line represents the manufacturer claimed freeway range of the example Zero SR, with the orange area representing its possible frontal area and Cd (drag coefficient) values. The blue area represents possible frontal area and Cd values, and corresponding ranges, for a motorcycle with the exact specifications of a Zero SR but the improved aerodynamics of a classical front fairing. Already this adds a nominal 50-60% increase in freeway range. The green area is the possible specification for an improved motorcycle design which further reduces aerodynamic drag by extending the fairing past the rider. Here the freeway range is increased by almost a factor of two over current designs and reaching over 300 km!

The Task

A rear fairing design does face one problem, it results in an increase in lateral surface area. Motorcycles are inherently sensitive to cross wind and turbulent circumstances because of their two-wheeled layout.[7][8] They can be pushed around or blown over by wind. Adding a larger, mostly flat surface will increase this sensitivity and could make the bike more dangerous in strong crosswind scenarios. Mitigating these effects became an integral part of testing my design and motivated me to experiment with an 'optimum efficiency' design alongside a shortened version, and a version with surface-area-reducing holes.

Successfully designing a rear fairing which can increase aerodynamic efficiency without excessively compromising stability would enable the construction of electric motorcycles with longer freeway cruising ranges and better high-speed performance. These improvements may help in motivating faster adoption of electric motorcycles, and thus allow those of us passionate about motorcycles to continue enjoying riding while preserving our environment and habitability of the planet.

With that overall goal in mind, my research sought to determine whether the aerodynamic efficiency of a motorcycle could be improved through the addition of a rear fairing. The ideal rear fairing would be positioned behind the rider and partially covering the rear wheel. It would be incorporated without compromising the stability of the motorcycle. In developing this design, I seek to answer questions about ways length and porosity of such a fairing would potentially affect motorcycle performance and stability. Of course, the end result should incite passion in the vehicle enthusiast as well as satisfy the logical consumer.

Conducting the entire design of a new aerodynamic component and testing it across all possible situations was, unfortunately, outside the scope of a thesis, so I necessarily set some limitations. Because the effects of aerodynamic drag are more prevalent at higher speeds, I limited my testing to freeway cruising ranging from 55 to 85 miles per hour (mph). I also limited the testing to a motorcycle traveling straight, as the dynamics/aerodynamics of turning are significantly more complex.[7][17] The consideration of stability was also limited to testing a crosswind scenario, where the effects of the additional fairing would be most prevalent. This thesis will track the process of developing and testing my rear fairing design within the above defined scope.

The first chapter, **Motorcycle Aerodynamics**, will begin by covering the principles of aerodynamics in a general sense and defining relevant terms and equations. It will then focus the discussion on motorcycle aerodynamics, applying the previously introduced concepts to outline the problems with current motorcycle design. It will provide a discussion of motorcycle aerodynamic stability in preparation for the modeling and testing of crosswind scenarios. This chapter will conclude with a detailed discussion of my rear fairing design.

The second chapter**, Computational Fluid Dynamics**, will introduce a means of modeling aerodynamic systems using a computer. It will form the basis of information required to show how computational fluid dynamics simulations can be used to test the performance of aerodynamic components.

The third chapter**, Models, Methods and Simulation Setup** will build from the information in the first two to explain testing methods applied during my rear fairing

design development process. It will chronicle the development and design choices made during the creation of the 3-dimensional motorcycle model, detail the specifics of the CFD simulation setup used throughout the testing process, and map out the logic behind the data I collected.

Chapter 4, **Results**, will discuss the results of my research through all three phases of the testing process. It will also acknowledge the limitations of my findings and provide a path for further testing.

The thesis will conclude with a discussion of the overall findings and possible next steps in the development of my rear fairing design.

Motorcycle Aerodynamics

Aerodynamics is a compound word - aero, meaning air, and dynamics, meaning motion: aerodynamics --the study of how air moves. Scientists and engineers have pursued the study of aerodynamics, in some form or other, for as long as humanity has been trying to harness the power of wind. Good aerodynamics has enabled boats to sail, windmills to spin, and planes to fly.[2] In the last two centuries, advancements in mathematics and physics enabled the development of a system of linear differential equations, the Naiver-Stokes equations, which mathematically capture the governing laws of fluid/gas mechanics. However, his system of linear differential equations, outside of simplified cases, has proved impossible to analytically solve, and oftentimes even impossible to completely computationally solve.[18]

This difficulty is reflected in the chaotic nature of medium to large scale aerodynamic systems. A small perturbation in the motion of air in one location can cause large scale changes in the systems resultant behavior. The old adage- a butterfly's wing beat in Africa can cause a hurricane in North America- captures the chaos of winds and airflows nicely. This unpredictability, even computationally, has led to the study of aerodynamics being affectionately referred to as a 'dark art'. Aerodynamicists never quite know how a system is going to behave before it is tested, and sometimes the results can be quite unexpected.

Despite this unpredictable nature, aerodynamics is not completely incomprehensible. There are ways of describing different aerodynamic states, and ways of predicting and understanding the aerodynamic behavior of a system.

Principles of Aerodynamics

One of the main tools in aerodynamic analysis is the distinction between two different types of flow: laminar and turbulent. Laminar flow is the fast, efficient flow state for air (and all fluids). It happens when the macroscopic motion of the system is uniform in one direction. Turbulent flow is the opposite, characterized by chaotic crisscrossing motion on a macroscopic scale. Picture a river. At the center of the river where the water is moving in one consistent motion, free of rapids and obstructions, the water will move relatively quickly, this is (almost) laminar flow. In white-water rapids or near the edge of the river where water swirls and slows into chaos, this is turbulent flow.

Another useful tool in the analysis of aerodynamic systems is the examination of differences in pressure throughout the system. Pressure generally refers to how quickly air particles are moving and how tightly packed they are. A high-pressure system will have air particles bouncing quickly off one another with little distance between. A low-pressure system will have particles that are further spaced apart and moving relatively slowly. This becomes important because a volume of air will always work to maintain uniform pressure: particles will automatically redistribute themselves throughout a volume to equalize any high- or low-pressure areas. This will manifest in an aerodynamic system as a force trying to move an object, along with the air particles, away from high pressure areas and into low pressure ones.

In a system where air particles are flowing around an object, the distinction between laminar and turbulent flow will be linked to high and low pressure. If air is moving backwards at a constant speed, or, conversely, if an object is moving forwards

at a constant speed through still air, the undisturbed flow will naturally be laminar. As the air encounters an object (or an object encounters the air) the air will usually maintain its laminar state and start to flow quickly and smoothly around the edge of the object. The pressure of the air will increase slightly about the object's leading edge, as it is forced to flow around. As the air rounds the sides of the object, two things can happen. If the transition from the front of the object to the sides and from the sides to the tail is gradual enough, the flow will maintain its laminar state and the object will pass with relatively low resistance. If the transition from the front to the sides, or the sides to the back, is too abrupt, the laminar flow will be disconnected from the edges of the object. At this point, there will be a "gap" or "pocket" of empty space between the laminar flow and the sides of the object. This gap, whether it be on the side or behind the object, will be in a low-pressure state, and thus the air will want to fill it to equalize the pressure. This rushing to fill the low-pressure space will cause the system to form vortices which will curl off the laminar flow and create a turbulent volume[4]. Because the system is still moving, the air peeling off in these vortices will never be able to fill the volume and equalize this pressure. The result will be a system with a high-pressure state in its leading edge and a low pressure, turbulent state behind. This will increase the amount of force being exerted on the object, as the high-pressure air tries to push it backwards, and low-pressure volume simultaneously tries to suck it backwards.

Figure 1.1 provides a simplified visual representation of these phenomena.

[4] Figure A.3 in the appendix is a snapshot from a simulation demonstrating this behavior in a two-dimensional system.

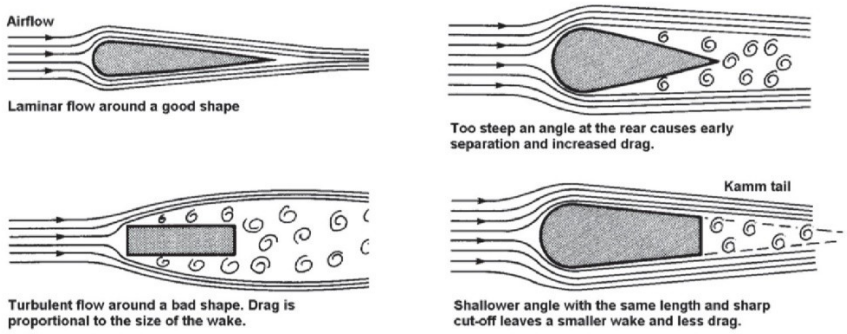

Figure 1.1: Depiction of Flows Around Various Objects.

This image is sourced from [8].

Here, laminar flow is represented by the parallel straight lines, while turbulent flow is the swirls. Observe that, as the air is breaking over the front of each object, the lines come closer together. This represents the increase in pressure occurring at the leading edge of the objects as they push the air out of their way. The shape of the object's leading edge, and everything behind, determines whether the laminar flow will disconnect from the edges of the object, from the back, or not at all. As illustrated, the most efficient objects will minimize the separation of the laminar flow and the formation of vortices and turbulence which are characteristic of low pressure.

As mentioned in the introduction, drag coefficient (Cd) is a measure of how aerodynamically efficient a shape is. More efficient shapes have lower Cds, and a shape with a Cd of zero would be essentially 'perfect', requiring no force to move it through the air. Cd is independent of the size of the object.

The measurement of the 'aerodynamic size' of the object is called frontal area. Looking at a colorful object head-on against a white wall, the surface area taken up by the object would be its frontal area. An object's frontal area and drag coefficient value determine the relationship between the speed at which the object (or the air around the

object) is traveling, and the amount of force required to move the object through the air: the force of drag. The relationship between these four values, and the density of the air ρ, is given by

$$F = \frac{1}{2} C_x A \rho v^2$$

Figure E.2: Equation for Force in Terms of Drag Coefficient and Frontal Area.

F is force of frag, C_x drag coefficient, A frontal area, ρ the density of air, and v velocity.

This equation will be used throughout this project. It assumes a squared relationship between speed v and force F. This relationship will be used later to test the performance of the simulation setup. Also, given the frontal area and density of air, this equation enables determination of the drag coefficient of an object by measuring the force on the object at known airspeeds. This approach will be used to measure the drag coefficient of the rear fairing design.

To better illustrate exactly what the rear fairing is designed to improve, the aerodynamic analysis tools can be applied to a normal, front-fairing motorcycle.

Motorcycle Aerodynamics

The aerodynamic problem that bedevils current motorcycle design comes down to us, the riders[5]. While front fairings can be as sleek and as smooth as designers imagine, they will inevitably end with some big, flat, gangly, meat-sack known as a person. And behind this person, both the torso and the legs, the motorcycle just ends. This means that the smooth laminar flow, which has been maintained around the front fairing, is quickly met with an uneven, flappy shape followed by a huge empty space

[5] Most of this discussion was inspired by [8] and [15]

where it devolves in a turbulent low-pressure mess. Figure 1.2 illustrates the scale of the problem.

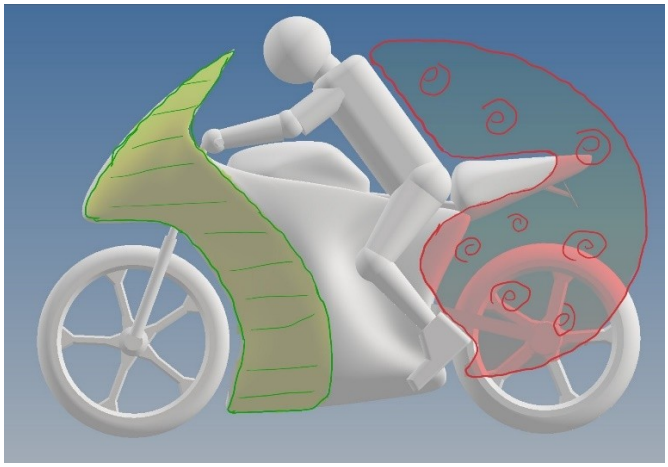

Figure 1.2: Simple Illustration of the Problem with Front-Fairinged Motorcycle Design. The green area with straight lines depicts the area of the front fairing over which laminar flow will be maintained, the red area shows the low-pressure, turbulent volume generated behind the motorcycle.

The only shape behind the rider designed to control the airflow is the rear cowl, but its effects are minimal. Motorcycles traveling at freeway speeds are hindered by the empty space behind the rider's torso and legs which creates a low-pressure volume that sucks the entire motorcycle-rider system backwards. Eliminating this low-pressure area, specifically behind the rider's legs, is the goal of my rear fairing design. However, there is more to aerodynamic performance than just drag coefficient.

I developed my fairing design to increase aerodynamic efficiency by considering how the basic principles of aerodynamics, including drag, high/low pressure, and flow types, adversely impact motorcycle aerodynamic efficiency. In addition, to ensure that my design did not result in unwanted safety issues, I had to understand and apply concepts related to motorcycle stability.

Aerodynamic Stability

One of the main concerns with my design was the possibility that the increase in the horizontal surface area of the motorcycle resulting from the addition of a rear fairing would increase the amount of horizontal force applied to the vehicle in a crosswind scenario. Intuitively, I was concerned that this scenario could cause the motorcycle to be easily blown over! To avoid making a catastrophic design flaw, I studied how aerodynamic forces acting on a motorcycle affect its stability. By focusing on principles of stability, I could begin to predict how the addition of my rear fairing might impact the behavior of a motorcycle in a crosswind scenario. This research also informed the type of data I needed to collect to test my predictions.

It is important to preface this discussion with an acknowledgement that the dynamics of motorcycle behavior are incredibly complex. Even conceiving of a motorcycle as simply a completely rigid body -- apart from the rotating wheels and turning handlebars -- does not eliminate complexities related to stability.

The motorcycle will still possess several degrees of freedom and the weird oscillatory, precession-y effects of rapidly rotating, gyroscope-like wheels. Entire books could be (and have been) dedicated to untangling the various properties that determine motorcycle stability.[7] The discussion and consideration here is limited to basic concepts of stability and their application to my model.

Understanding the stability of an object in motion can be simplified to determining how the object reacts when force is exerted on it. An object's reaction to force is a function of three variables. First, there is the magnitude of the force (how hard the, in this case, air, is pushing on the motorcycle). Second, the direction in which

this force is being applied (is it being applied backward, up, down, sideways?). Lastly, the “location” in which the force is applied relative to the center of mass of the object, or its axis of rotation, will impact how the object reacts.

The center of mass of an object, more colloquially called its balance point, is defined as the point at which, if a force were applied, the object would undergo only linear acceleration and not angular acceleration. Picture a rubber ball floating, halfway submerged in a still pool of water. If one were to push on the ball with their finger right at the center of its ‘equator’ pushing it directly backwards, the ball would only move directly backwards. If they were, however, to push on the ball above the equator but still directly backwards, it would still start to move backwards (linear acceleration) but also rotate under their finger (angular acceleration). That is because the ball (assuming its uniform) has a center of mass right at its geometric center. The first force was applied directly in line with its center of mass (if they had had a needle on the end of their finger, it would have gone right through the ball’s center), thus the ball only linearly accelerated away from them, while the second force was applied out of line with the center of mass, so the ball moved and rotated. This same concept can be applied to aerodynamic force.

Continue picturing the ball floating halfway out of the water, but instead of pushing on it with a finger, the person blows air on it through a straw. If they were to blow through the straw and aim it exactly at center-of-the-equator point, they could again cause the ball to move directly backwards. Similarly, if they aimed the straw and blew towards the top of the ball, it would move away from them a little less, but also start to rotate. In terms of the ball’s reaction, it does not matter whether it is being

pushed by a bunch of tiny little forces from air molecules bouncing off its surface or by one big force applied at their fingertip. All that matters is the average direction of the total force, the magnitude of the total force, and the average center of the position with which this force was applied relative to the center of mass of the ball.

Of course, not all objects are free moving balls. An object that is locked to rotating about a fixed axis, like a door on hinges, will behave differently when force is applied. Even though forces could be applied in any of the cardinal directions, the only force which will induce a motion in a door is one about the axis of rotation: if one pushes a door up, or pushes on its edge directly towards the hinges, it will not move.

The numerical measure of how much a force is going to angularly accelerate (rotate) an object is called torque. Limiting the consideration to a force exactly perpendicular to both the axis of rotation and the line connecting the center of mass to the point at which force is being applied (this condition will be met throughout this thesis) torque is given by

$$T = rF$$

Figure E.3: Equation Relating Torque to Force Magnitude and Distance of Application from Axis of Rotation or Center of Mass.

with *r* the radius, as in Figure 1.3, and *F* the magnitude of the force. It is important to note that *r* and *F* both have equal weight, so reducing the radius by 25%, but increasing the force by 25%, results in no change in the perceived toque. This will be important later.

The same concepts introduced in the discussion of balls and doors can be applied to determine how aerodynamic forces will affect the motion of a motorcycle moving down the freeway. A motorcycle will react to force consistent with both the center of mass principle, as illustrated by the free moving ball example, as well as the fixed axis reaction, as exemplified by the door hinge example[6]. This is the case because when a horizontal force is applied to a motorcycle, the wheels can act like the hinges of a door, causing the bike to want to roll over on its side. At the same time, because the front wheel can turn, a horizontal force can also cause the bike to rotate around its center of mass. To better illustrate what to look for in a simplified consideration of motorcycle stability, I discuss three different potential aerodynamic forces.

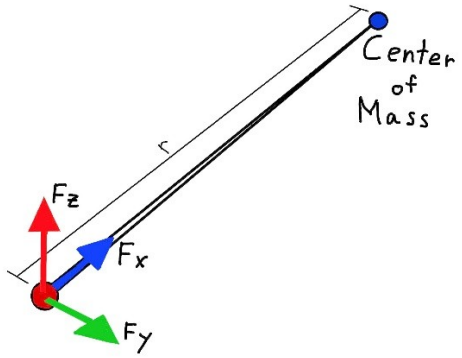

Figure 1.3: Forces Being Applied a Distance *r* From the Center of Mass

Each colored arrow represents a force vector in one of the cardinal directions. In this depiction, they are all being applied to the same point, the same distance *r* from the center of mass, but in practice each one will have an individual location.

As shown in Figure 1.3, the forces of air particles bouncing off the surfaces of the motorcycle can be represented with three single aerodynamic force vectors (like representing the force of air blown on the ball as a finger) -- one pointing in the X

[6] This discussion was inspired by sections of [7] and [8].

direction (backwards), another pointing in the Z direction (upwards) and a third pointing in the Y direction (horizontally) at a set distance from the motorcycle's center of mass.

The force in the X direction (backwards), pointing directly through the center of mass, is the force of drag discussed in Chapter One. This is what will be measured for the force of air pushing the motorcycle backwards and used to calculate the drag coefficient.

The force in the Z direction (upwards) is usually called lift because it is what is working to lift the motorcycle off the ground. Lift plays a noticeable role in determining motorcycle stability.

When a motorcycle's tires contact the road, they generate fiction, usually called grip. The more grip they generate, the less likely they are to slide. Because the connection between the tires and the road is critical to the ability to control the motorcycle, it is very important a bike be designed to generate as much grip as possible. The amount of grip generated is dependent on several factors, but the only one which will be affected by the aerodynamics is the magnitude of force pushing the tires into the ground. More force means more grip. That is where lift comes in.

If the motorcycle is generating lift, that is taking weight (force) off one or both tires, thus reducing the total amount of friction they can generate with the road. No matter what, it is best to reduce the overall magnitude of the lift vector to increase the rider's control and thus the motorcycle's perceived stability. However, the location at which this vector is being applied must also be considered. If the lift vector is acting upwards *in front* of the center of mass, the induced rotation lifts the front wheel off the

ground and presses the back-wheel into the ground. If the same lift vector acts *behind* the center of mass, it induces the opposite rotation, thus pressing the front wheel into the ground. Since the front wheel is the only means for controlling the bike, it is preferable that any rotational force resultant from lift be pushing it into the ground.

The effects of force in the Y direction[7] (horizontally), introduced in the discussion of stability above, require further in-depth discussion. As a result of the motorcycle's tendency to behave both like a door and like a ball, the magnitude of this force must be considered alongside two different radii, the one to the center of mass, and the one to the ground.

These two radii will be the determinants of two different behaviors induced by a crosswind: the motorcycle's tendency to roll over and its tendency to yaw out of the wind. The tendency to roll over will be determined by the radius to the ground since the axis about which the 'door hinge' type behavior will occur will be through the tires' point of contact with the road. The tendency to yaw out of the wind will be determined by the application of the crosswind force relative to the radius to the center of mass. An increase in either of these effects will be detrimental to the perceived, and actual, stability of the motorcycle.

With these principles in mind, I introduce my concept rear fairing design, illustrated in Figure 1.4.

[7] If the motorcycle were traveling straight in still air (no crosswind) the magnitude of this force will be zero, so this discussion pertains only to the crosswind scenarios.

My Concept Rear Fairing Design

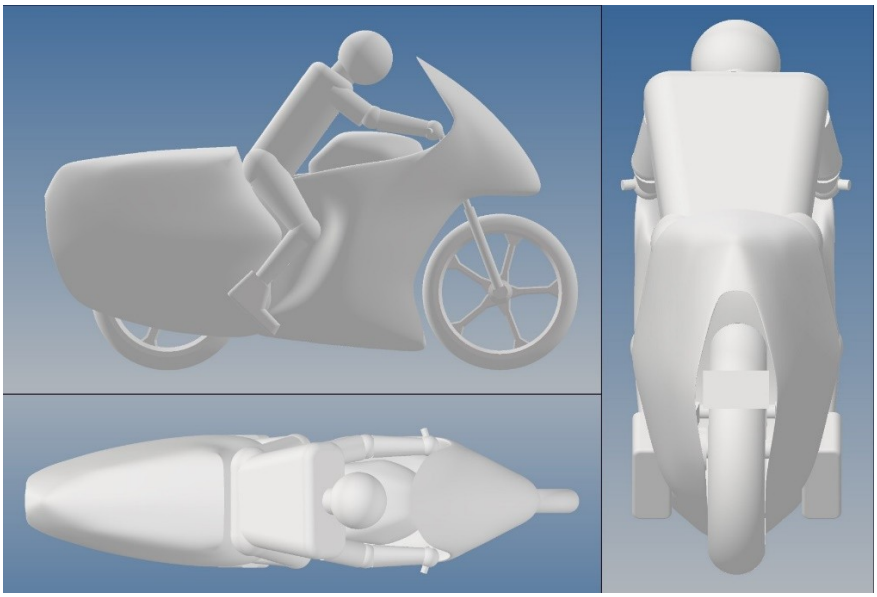

Figure 1.4: Overview of My Concept Rear Fairing Design

This figure depicts my rear fair design mounted to a front-fairinged motorcycle.

As discussed in Chapter One, the main problem with current motorcycle designs aerodynamically is the sharp cutoff to empty space directly behind the rider. This cut off introduces turbulence and creates a volume, or pocket, of low pressure directly behind the rider, effectively 'sucking' the whole system backwards. My design aims to completely eliminate this low-pressure pocket behind the rider's legs.

Specifically, air will be moving around the front fairing in steady but accelerated laminar flow. The goal of my rear fairing design is to encourage the continuation of this laminar flow over the rider's legs, allowing it to stay connected along this rear fairing until a sharp cutoff to a much smaller area behind the fairing[8]. By encouraging this laminar flow, the fairing should reduce, if not eliminate, this low pressure, turbulent

[8] A design like the Kamm-tail in figure 1.1

volume behind the rider's legs, thus alleviating some of the "sucking" effect and increasing aerodynamic efficiency.

However, because the design increases the horizontal surface area, addition of the rear fairing will result in an increase in the total amount of horizontal force that is applied to the motorcycle in a crosswind scenario. The additional force raises stability concerns, specifically with yaw (the tendency to turn away from the wind) and roll (the tendency to be blown over). The roll case is clear cut -- this design will probably increase the risk that the motorcycle could roll over in a crosswind. The yaw case is more complicated. Since the fairing is increasing the surface area behind the rider, the added force applied to the rear fairing will be *behind the center of mass*. While the horizontal force on the front fairing (always centered in front of the center of mass) is causing the bike to yaw away from the wind, the force on the rear fairing will counter this effect and cause the bike to want to yaw into the wind. This means the addition of the rear fairing will take the total center of horizontal force and move it backwards. Understanding whether the increase in horizontal force outweighs the shifting backwards of the total center of force, i.e., causing the bike to tend to yaw less into the wind, or whether these effects are more or less brought into balance, required measuring the extent to which my design moves the center of force backwards. Taking these measurements was an important step in the testing process but, before I could test my design and take these measurements, I had to choose my modeling tools.

Computational Fluid Dynamics

Computational fluid dynamics (CFD) is the blanket term for, as one might expect, modeling the motion of fluids using a computer. In addition to being used to model the motion of fluids, CFD is often, if not usually, used to model the behavior of gases. It's not a misnomer though. Gases and fluids have almost the same properties. In both states, molecules are free to move and flow in any direction they want. The main distinction is that, in a fluid, these molecules are packed tightly together and cannot be compressed, while in a gas they bounce around with ample space in between them and can be compressed. Interestingly, many gasses, including air, at low states of agitation, can be modeled as incompressible fluids. Regardless, compressible vs incompressible is a relatively minor distinction for a computer so, as I will do throughout the rest of this thesis, air is regarded computationally as a fluid and is referenced as such.

The ability to model the behavior of fluids in a computer is a relatively recent development but has become key to modern vehicle design.[1] Thirty years ago, testing an aerodynamic component would have been a major undertaking. After educated guesswork in the design process, engineers would have built a scale model and placed it in a wind tunnel[9]. Alternatively, engineers might have sent a full-size model out into the real world to be tested by some poor brave pilot. This was an awfully expensive and time-consuming process, seriously limiting the extent to which proper aerodynamic testing could be performed.[1] The advent of CFD changed that.

In addition to quickly becoming much less expensive (although still requiring a supercomputer) than traditional testing methods, over time CFD technology improved

[9] A wind tunnel is a large-living room-sized tunnel with enormous fans on one end to create artificial high-speed airflow throughout the entire space.

and computations could be performed faster. Accordingly, CFD emerged as a readily available alternative means of quickly and safely testing any conceivable scenario. Want to test a racecar at 20 then 220 mph? Just change a single number and hit enter. Wait an hour (or five) and boom, CFD generates all the data one could want. No more patting a test-driver on the back and assuring him “I’m pretty sure this will work”. Today the vast majority of aerodynamics testing on major vehicle components is performed using CFD.[1][11] All this is not to say that CFD has eliminated the need for real world testing. In the process of bringing a design from a sketch to a full-size vehicle, time in a wind tunnel is still necessary, but now it is used mainly to confirm the predictions of CFD simulations.

The real beauty of CFD as it pertains to this project, though, is that it has even more recently become accessible to almost anyone. In the last five years, leaps in the processing power of consumer-grade computer hardware have eliminated the need for a warehouse-sized supercomputer to quickly run complex CFD simulations. CFD testing can be done on a powerful desktop. In testing my concept fairing design, I was able to follow the exact same initial process, with equivalent tools, as Ducati engineers designing their next race bike. I explain this process in detail in the Methods section. However, it is important to first discuss how CFD simulations work and how to set them up in a way that will yield useful results.

CFD Theory

As mentioned in the aerodynamics section, the Naiver-Stokes equations mathematically represent the laws governing the behavior of a fluid, however, they are extremely difficult to computationally solve. CFD simulations skirt this problem

because, rather than trying to solve theses equations and predict the behavior of a fluid, they seek to model, in simplified a simplified manner, the actual behavior of the fluid based on rules defined by these equations. They do so in several steps[10].

Every 3-dimensional CFD simulation starts with a defined volumetric area. The computer needs to know "in here there is fluid, everywhere else, there is no fluid." Then, properties can be assigned to the fluid in this volume. For example, one could model air at a set, uniform, temperature and pressure. The next step is to define any non-fluid objects sharing the space. This is usually done by creating a 3-dimensional model using Computer Aided Design (CAD) modeling software. These models are then loaded into the volume, and each material in the model is assigned a set of properties defining how it is going to interact with the fluid (is it solid? How much friction will it generate with the air? etc.). For my project, I loaded a 3-dimensional model of a motorcycle into a volume of air.

The computer will then simplify the volume, both solid and fluid parts by subdividing it into smaller volumes called cells. Each of these cells will individually know whether it is a fluid cell of a solid cell and will be assigned a state. In the case of solid cells this state is simply 'being solid'. For fluid cells, this state corresponds to the average direction and magnitude with which air is moving within that cell. So, a cell might know that it has air in it moving 70 mph straight backwards. A depiction of the cells as applied to a CAD model is shown in Figure 2.1.

[10] This discussion was inspired by [4],[14] and my own learning process.

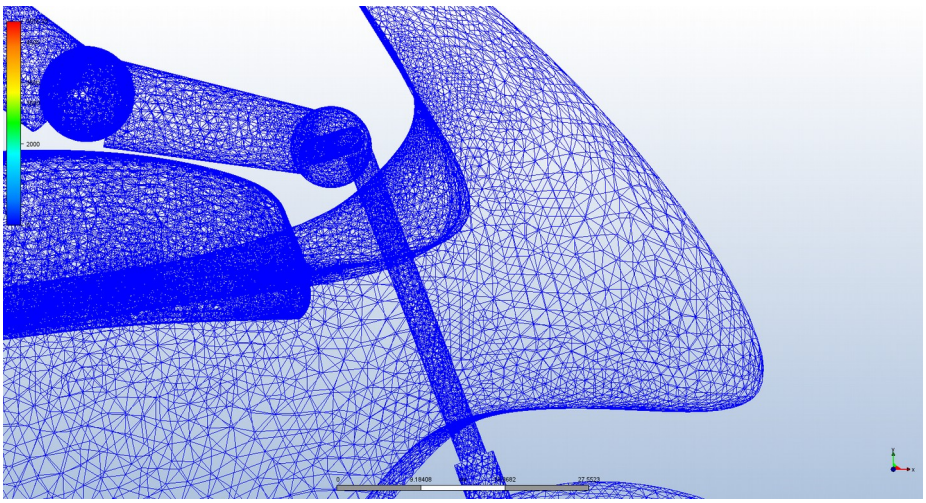

Figure 2.1: Solid Section of a CAD Model After Being Subdivided into Discrete Cells. Notice how, with sufficiently small cells, the computer can effectively mimic the curved sections of the fairing with flat geometries.

The computer runs the simulation in discrete timesteps, meaning fluid will not continuously move from one cell to the next. Instead, at each time step, each cell will interact with its neighboring cells and fluid will jump from one to the next based on the states of the interacting cells. The ‘70 mph backwards’ cell will tell the cell behind it ‘you now have fluid in you traveling 70 mph backwards’. During these jumps, fluid will ‘bounce off’ the solid cells. Measurements of the aerodynamic forces on a motorcycle will be taken during interaction between the fluid cells and solid cells.

Determining how finely the computer should subdivide the volume is called ‘mesh sizing’. A finer mesh (one with more, smaller cells) will yield a more accurate result, but will require more computations at every timestep. Similarly, deciding how many steps the computer should calculate determines how long the simulation will run.

The final step in setting up a CFD simulation is actually getting the fluid to move. This is done by assigning boundary conditions.

Boundary conditions tell the computer what is going to happen to fluid when it interacts with the faces of the volume. Usually, these are divided into inlet, outlet, and wall conditions. Inlet conditions determine how fluid will flow into the volume. There are myriad different ways to do this, but for the purposes of this research I only needed a uniform, continuous inlet of fluid traveling in a set direction at a set speed (like the enormous fans blowing air into a wind tunnel). The outlet conditions are the opposite; where does the fluid leave from? Without an outlet condition fluid would be continuously pumped into a closed volume yielding no flow. A common outlet condition is one in which one wall of the volume is assigned zero pressure. Any fluid that interacts with this wall will essentially 'fall' through it with no resistance. Like a portal to the limitless void. This allows the inlet condition to continuously "push" fluid into the volume, while the displaced fluid falls out the opposite end. Finally, boundary conditions for the borders or walls of the volume which are not inlets or outlets must be assigned. Assignment of wall conditions is highly dependent on the nature of the system being modeled. If left unassigned, the walls will default to still air, but this can cause problems as the moving air from the inlet will be slowed down by the still air on the walls resulting in a volume of slow moving, slightly turbulent air around the edges of the simulation space. To avoid this, the walls are usually assigned to have air moving with the same speed and direction as the inlet condition.

Practical Implementation

There are some special considerations that inform the setup of a CFD test space that is being used specifically for aerodynamic testing. The first is deciding whether to model air as a compressible or incompressible fluid.[2] Modeling air as a compressible

fluid is more computationally challenging because the system also must store and compute information about the density of air in each cell. However, air only behaves like a compressible fluid at high extremes of interaction. In fact, it has been shown that at max air speeds of less than 250 mph, air can be modeled as an incomprehensible fluid with an error of less than 3%. At 150 mph, that error is reduced to 1%.[10][11] So, when dealing with lower air speeds it can be more computationally efficient to model air as incompressible with a very minor loss of accuracy.

The second consideration is the number of timesteps over which to run the CFD simulation. At the first timestep, the air filling the volume will be stagnant. Over the next several timesteps, the inlet will slowly work to push moving air into the system, which will eventually shove the stagnant air out of the outlet. It can take several iterations for this to happen, and several more for the flow to stabilize and become "fully developed". Flow is fully developed when the flow through the entire volume is, apart from the disturbances caused by the model itself, constant. To test an aerodynamic design at a particular speed, the flow in the volume must be fully developed at that speed. Thus, it is necessary to run the simulations for long enough to achieve this state.

The third consideration is the size of simulation volume or, more specifically, the distance between the CAD model and the walls. If the model is too close to the walls of the space, the fluid being deflected around it will interact with the edges of the volume. This can create a compounding effect where the fluid is being squished between the wall and the model, making it more difficult for fluid to flow. The CAD model acts like a clog in the virtual pipe which will cause the system to measure a higher overall force acting on the vehicle than would occur in the real world. Similarly,

if the model is too close to the outlet wall with a zero-pressure condition, the outlet wall will ‘suck’ the wake away. In the case of a motorcycle, this would eliminate the effects of the air trying to “fill in” the low-pressure pocket behind the rider and thus unrealistically eliminate the negative effects of this low-pressure area. In both cases, an additional side-effect would be a lack of ability to properly observe the flow around the model because the computer will not simulate anything beyond the limits of the simulation volume.

By modeling the flow of fluid around an object, CFD software can generate both numerical data (measurements of the aerodynamic forces on a CAD model at each simulation step) and 3-dimensional images showing the flow of fluid around an object. These images come in different forms depending on the information displayed, but one of the most illustrative is a particle path trace.

How to Interpret CFD Images

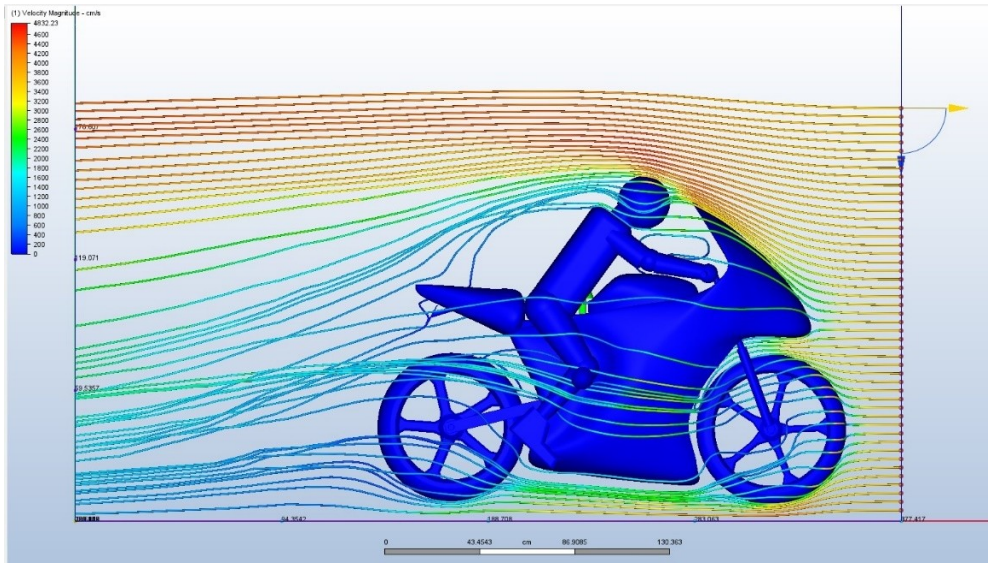

Figure 2.2: Particle Path Trace of the Flow Over a Motorcycle.

This image was collected during the testing process. It depicts the flow of a 65-mph headwind over a front-fairinged motorcycle.

I used images like the one shown in Figure 2.2 throughout the testing process to qualitatively understand how various front and rear fairing designs were affecting the aerodynamic behavior of the motorcycle. Each ribbon in this image follows the path of a single particle as it moved through the simulation volume. The color of the ribbon corresponds to the particle's speed at each point of its journey. The parallel orange lines on the right-hand side of the image reflect the laminar flow entering the simulation volume from the inlet condition. From there, they impact the front fairing and accelerate as they are compressed around it. This image also illustrates the problems with current motorcycle design discussed in the Motorcycle Aerodynamics section. In the space behind the rider, all the particles were slowed down, changing from red and orange to shades blue. The parallel lines of laminar flow are lost to the crossing paths of

turbulence, and, particularly right behind the rider's knee, particles are being greatly slowed as they are sucked into the low-pressure area directly behind the motorcycle. This is what my rear fairing design is meant to eliminate.

To see whether it actually works, I had to test it. In the next section I build off this discussion of CFD to describe in detail how I tested my fairing design against a front-fairing motorcycle like the one pictured in Figure 2.2.

Models, Methods and Experimental Setup

The objective of the testing process was to determine whether the drag coefficient of a motorcycle could be reduced without compromising stability through the addition of a rear fairing. At the core of this investigation is a comparison, and leveraging this comparison enabled the collection of meaningful data without the burden of creating a CAD model and CFD simulation setup which *exactly* mimicked the real-world. Instead of simply making a model of the rear-fairing concept and testing its performance compared to the real-world performance of a front-fairing bike, I constructed a virtual representation of a front-fairing bike, then added the rear fairing. This approach enabled me to compare the performance of the two within the CFD simulation space. It was, of course, necessary to ensure the performance and aerodynamic behavior of the standard front-fairing model matched expectations for real-world behavior, but the match needed only be 'good enough'. Once that was achieved, the comparison within the CFD world benefited from easy control of all variables outside the changing rear section of the model.

Throughout this testing process both quantitative and qualitative data were collected. The qualitative data amounted to force magnitudes and locations for the X, Y, and Z directions resulting from airflow incident on the motorcycle models. These were used without manipulation for stability analysis or converted into drag coefficient or range estimates. The qualitative data was collected using particle path traces and other means of visualizing the flows within the CFD software. The qualitative and quantitative data was combined to gain an understanding of the overall aerodynamic behavior of the models.

The models were constructed using the CAD software suite Autodesk Inventor, and the CFD simulations were run in the accompanying Autodesk CFD. Both sets of software are commonly used by industry professionals for the design and testing of aerodynamic components.

With the basics of the testing methods outlined, details highlight how the CAD models were constructed and the parameters/test setup used in the CFD simulations. To begin, there follows a discussion describing the properties of the basic motorcycle model and outlining how it was evolved and modified throughout the testing process.

Making a Motorcycle

When creating a digital model for CFD testing, it is standard practice to simplify the model and generally ignore details.[1][14] As discussed in the CFD section, every additional competent and surface in CAD model means more calculations for the computer to perform at each timestep and thus increased computation time. The goal, then, when creating a CAD model for CFD use, is to only include the components that are going to have a significant effect on the aerodynamics of the vehicle. Things like wing mirrors, brake levers, wires, gauges and even front and rear brake discs have a minimal effect on the aerodynamic properties of the vehicle and are often eliminated in models.

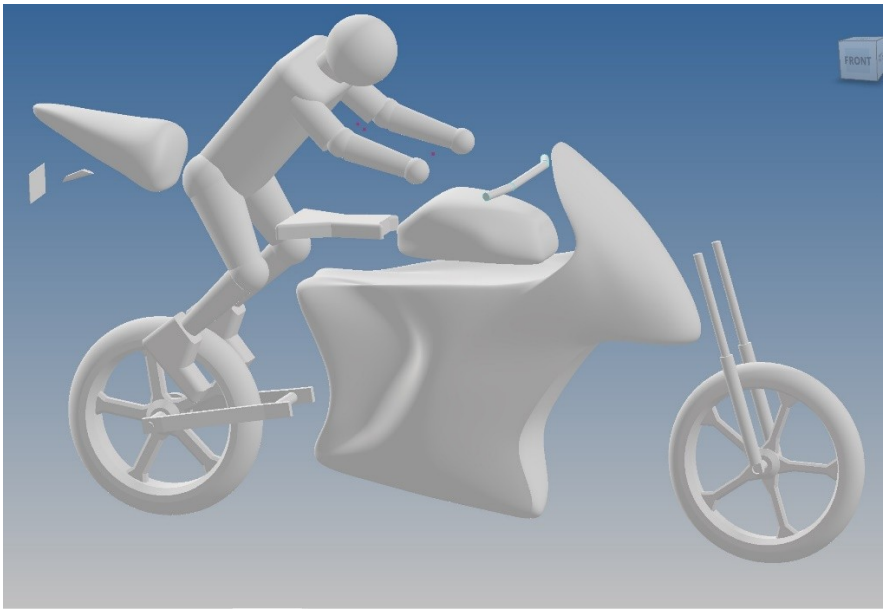

Figure 3.1: Exploded View of Standard Motorcycle

Figure 3.1 is an exploded view of the motorcycle model I created to represent a standard front fairing motorcycle. It features a main body section consisting of the front fairing and a representation of the internal structure. Connected to this are the front wheel and front fork, handlebars tank, seat, the rear wheel, and a little bit of the assembly which mounts the rear wheel to the body. It also features a fully rendered person, the rear cowl and license plate. The size of most components (wheels, 'frame', tank, seat, forks, handlebars and swingarm) in this model are identical to measurements of an existing motorcycle (my 2003 Triumph Bonneville). The front fairing design is a sort of 'average' of those found on several sport-touring style motorcycles combined to create a basic front fairing shape. The rider is modeled after myself, and positioned in an average comfortable riding position. I took measurement of each limb, both length and radius, and digitally reconstructed them into the sort of mannequin pictured above. The head is sized like a helmet.

This model, while obviously simplified, retains the most significant aerodynamic components and the overall volumetric shape of a fairinged sport motorcycle. The most impactful simplification in this model comes from the main core+fairing component which, in a real motorcycle, would comprise the front fairing and frame, along with the drivetrain (batteries, electric motors, computers etc.) and all other internal components. In this case it is modeled as one continuous sealed object. Sealed being the notable simplification because in a real motorcycle the front area (shown here) would be open with ducts and paths for the air to flow into the internals of the bike to be used for cooling of the batteries and electric motors. The difficulty when translating something like this to a CAD model is that the model then needs all the internal parts (the battery, electric motor, and frame) represented as components. This would have resulted in a model with two or three times as many components and therefore a related multiplication to the number of surface interactions calculated at each timestep of the CFD simulations. To avoid this additional processing work, internal parts are not modeled.

This simplification will, to some extent, compromise the accuracy of the model because the model will not benefit from the effects of drag reduction attributed to air flow through the internals of the motorcycle. Results will not be greatly affected because 1) this reduction in drag will affect all models equally and 2) the air which would be allowed to flow through the motorcycle would exit either right ahead of the driver’s knee, or out the back of the motorcycle. In either case, this would not result in a substantially different flow around the overall system. The effects of this simplification will be reflected in a slightly higher measured drag coefficient compared to real-world

values. The benefits of this simplification in terms of simplicity will far outweigh any losses in overall accuracy.

Starting from this principle design, seven more models were created in total. To keep track of them all, I introduced an intuitive naming system. This first model, without the rear fairing, was called NF1 (no fairing 1). From NF1 was spawned a model featuring the first iteration of the rear fairing design, F1 (fairing 1). Both the front and rear fairings were eventually slightly redesigned (more on that later) to create the models NF2 (no fairing 2) and F2 (fairing 2). Note that model F2, and all subsequent models, featured the NF2 front fairing. In between these and the model with the most complicated name there was an iteration with the redesigned front fairing but the original rear-fairing design, this I called N2F1. Finally, based on the F2 design, I created three more variations on the rear fairing idea which were used to test two properties: length and porousness. These were called SF (short fairing), FH (fairing with holes) and SFH (short fairing with holes). Figure 3.2 shows the models F2, SF, FH and SFH.

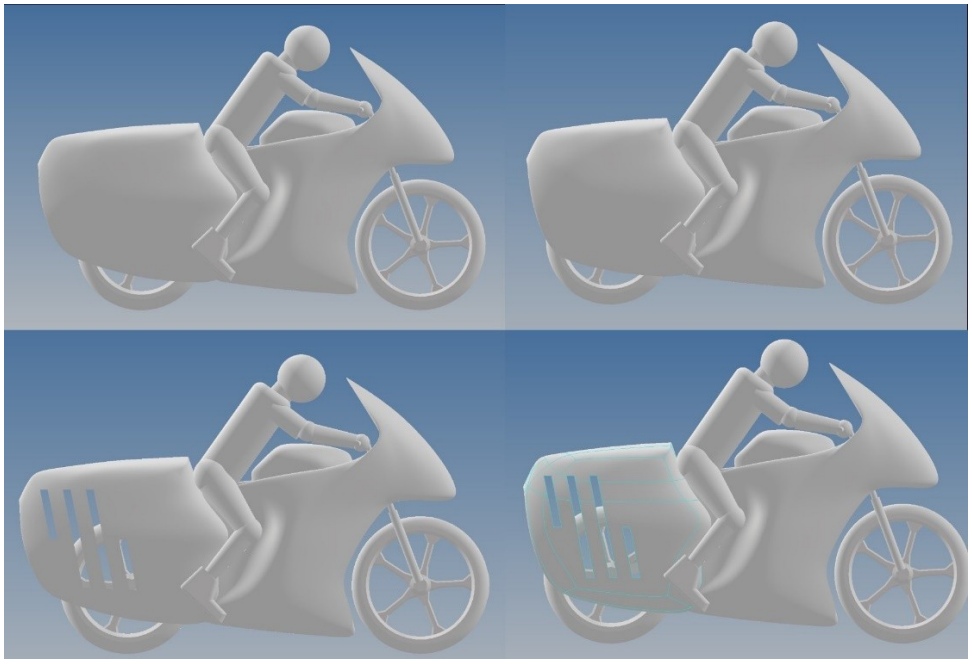

Figure 3.2: Models F2, SF, FH and SFH

Models are depicted left to right, top to bottom

The first and most important thing to explain about the creation of these models is that the ONLY differences between F1 and NF1 or F2 and N2F1/F2/SF/FH/SFH were the removal of the rear cowl, its replacement with the rear-fairing, and the corresponding relocation of the license plate. Thus, the only property of the system changed was the existence of a rear fairing in place of a rear cowl. The placement of all other components, including the placement and position of the rider, were kept identical.

Another important note is that the frontal area of these models was kept constant both through the redesign from NF1 to NF2, and regardless of the rear fairing or cowl. The rear fairing design exists entirely in the ‘shadow’, so to speak, of the front fairing

and rider. In other words, when you look at the models head-on, you cannot see any part of the rear fairing. The calculated frontal area for all models was 0.6945m^2 [11].

The redesign of the front fairing from NF1 to NF2 was very minor. Nothing about its overall size, shape, or position was changed. The only changes came because of observations about airflow in the first round of testing. I noticed that the very leading edge of the lower section, right near the 'air intake' was angled too sharply inward and was followed by a flatter section leading towards the rider's legs. This was causing the very front of the faring to cast a wake and disconnect the laminar flow from the rest of the fairing's length. In the redesign, I simply changed the shape of this panel, as depicted in Figure 3.3, to make it a continuous slope from the edge of the intake to where it meets the rider's legs.

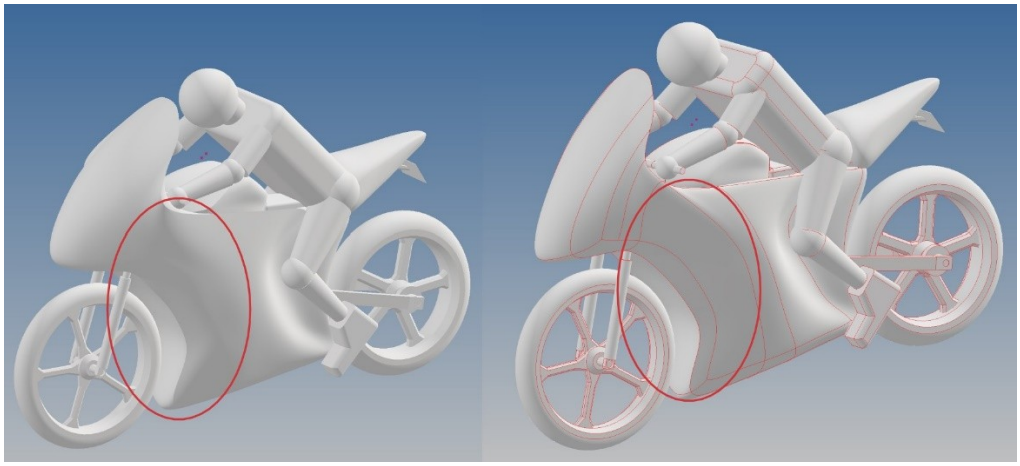

Figure 3.3: NF1 vs NF2

NF1 on the left, NF2 on the right. The red circle highlights the redesigned area. Notice the smoothness of the shadow in the NF2 compared to the same surface in NF1. These photos were not taken from the exact same perspective.

The redesign of the rear fairing was similar, and again motivated by observations in the data collection phase. I did not change the overall length, height, or

[11] The frontal area was calculated with Autodesk Inventor.

position, but increased the width at the rear (particularly on the upper section) so the faring was overall less curved inward at the back. This was again to mitigate observed separation of the laminar flow from the body work resulting from a rapidly tucking tail section. This redesign is illustrated in Figure 3.4.

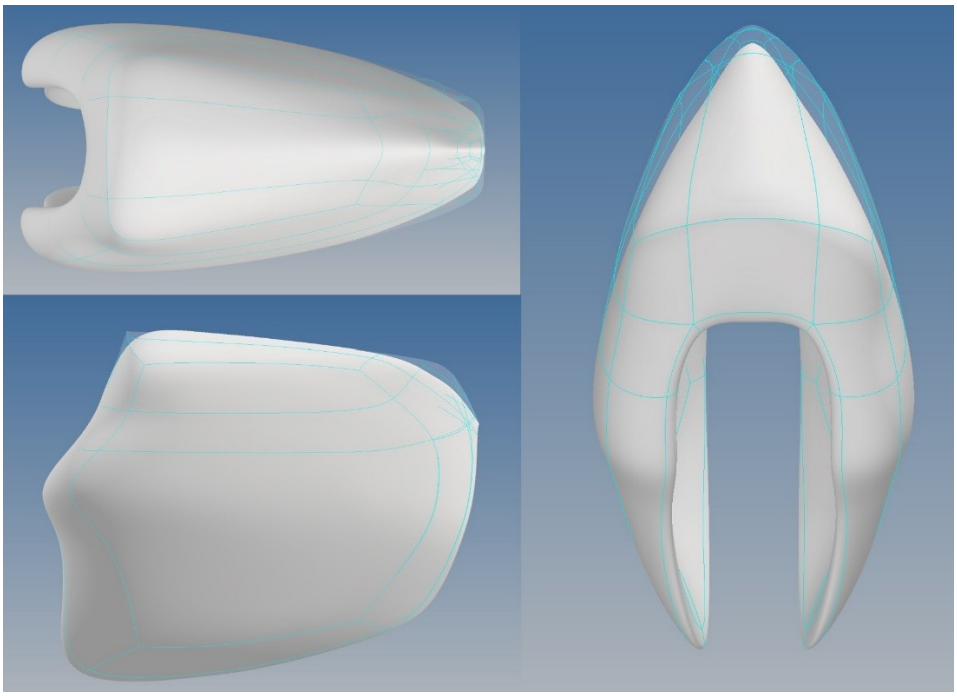

Figure 3.4: Changes Made During the Redesign of the Rear Fairing

The original (F1) fairing is depicted by the solid ceramic-colored shaped. The version 2 (F2) fairing is depicted over F1 with the transparent shape and blue lines. The overall length, height and width were maintained, but the fairing was widened at the rear.

Creating the shortened version of F2, SF, was a slightly more complicated process. The entire rear section of the fairing was shortened by 5 inches (13cm). To eliminate other sources of performance variation, the taper of the fairing was kept the same (see Figure 3.5).

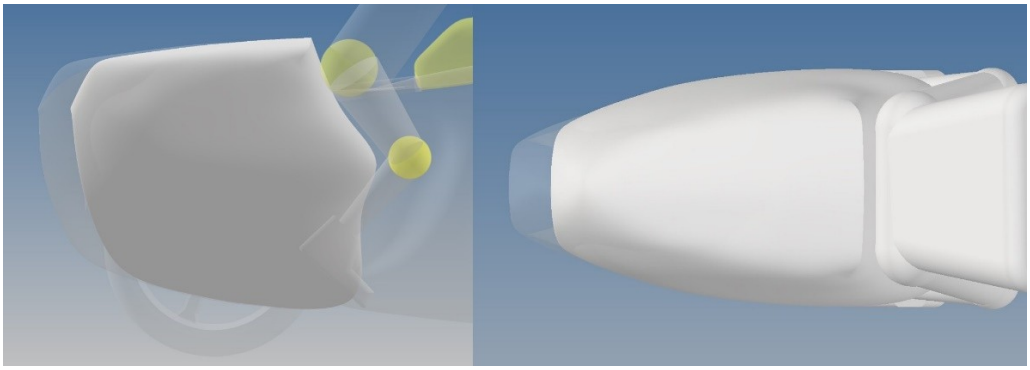

Figure 3.5: F2 vs SF

The shortened fairing is depicted here by the ceramic-colored shape, with the longer (F2) fairing is depicted by the transparent volume. The left image shows how the fairing was shortened by 5 inches. The right image shows how the taper of the fairing was maintained.

This led to a slightly wider opening at the back. Otherwise, the fairing design was unchanged. From F2 and SF, their sister models FH and SFH were created. The design of the 'holes', vertical rectangular sections symmetrically cut from the faces of the fairing, were in some ways arbitrary. Their shape and placement were based mostly on looking at the rear wings of Formula 1 cars and educated guesses as to what design might improve performance in the crosswind tests without reducing the effectiveness of the fairing. The design of the holes is the exact same in FH and SFH, but they are necessarily moved forward in the SFH model. With an understanding gained of the CAD models' properties, a description follows of the CFD setup used for testing.

Making a Virtual Wind Tunnel

I used two CFD simulation setups in the testing process, one for measuring drag coefficient and lift in normal freeway cruising conditions, and one for measuring horizontal forces and lift in a crosswind scenario. Both setups consisted of a large rectangular 'wind tunnel' with the model centered, near the inlet, and close to the

ground. By carefully choosing inlet, wall and outlet conditions, this virtual wind tunnel could simulate a flow of air moving at any given speed over the model[12].

The model was placed close to the bottom of the wind tunnel to mimic ground effects[13] and positioned close to the inlet to allow ample room for the wake to be seen while avoiding effects of flow disappearing out the 0-pressure outlet. As discussed in the CFD section, it was important to ensure that the tunnel was big enough to avoid the flow around the model being affected by wall interactions, thus, the wind tunnel, as shown in Figure 3.6, was 3m (10ft) wide, 3m tall and 5m (16.4ft) long.

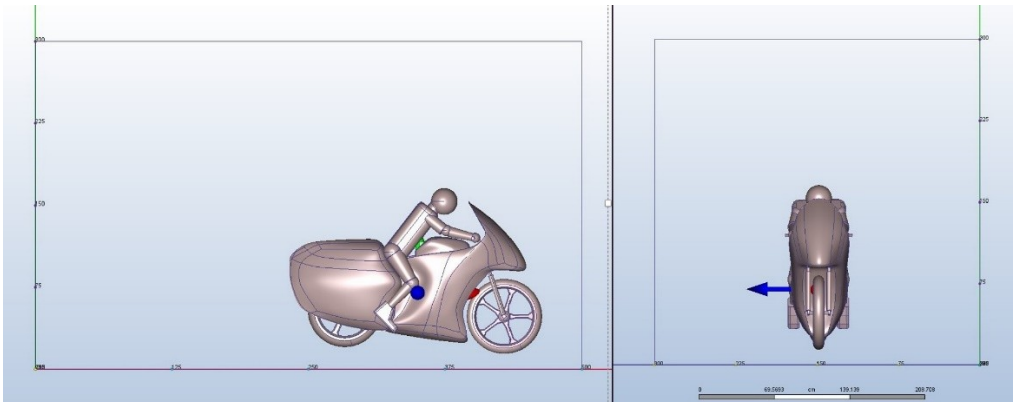

Figure 3.6: Wind Tunnel Design

The wind tunnel is depicted here by the fine black rectangles encasing the F2 model. The left shows the long face of the tunnel, with the model pushed close to the inlet. On the right the model is depicted from the front.

In testing of the normal freeway cruising performance, the models were placed exactly perpendicular to the inlet wall. To enable checking of consistency, both for the model performance and the behavior of the testing step itself, each model was tested in this setup at four different 'freeway' speeds: 55, 65, 75 and 85 mph (88.5, 104.6, 121 and 137 km h respectively). The inlet and wall condition were set as uniform with air

[12] There is no distinction between a model moving through air, and air moving over the model.
[13] Ground effects are interactions between the flow around and motorcycle and the ground

moving at the selected speed in the negative x-direction, and the outlet condition was set to 0-pressure.

For the testing of a crosswind scenario, a single wind speed and crosswind speed were selected. To simulate the aggregate flow of a vehicle moving forward with a crosswind, the vector sum of the two wind speeds and directions was calculated to determine the magnitude and direction of the resulting flow.

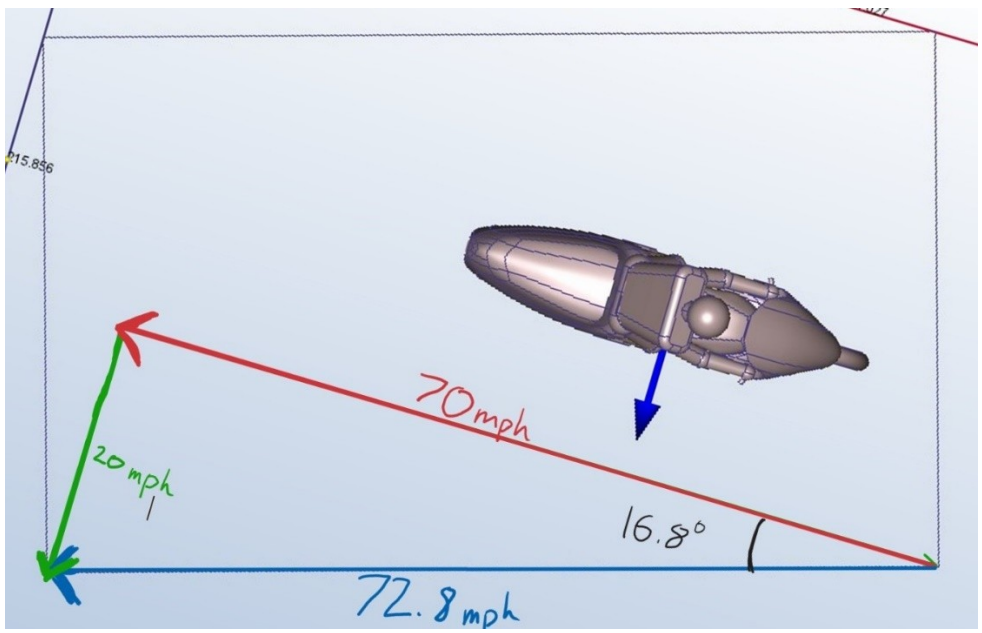

Figure 3.7: Wind Tunnel Adapted to Crosswind Scenario

The colored vectors depict the summed windspeeds of 70 mpg backwards and 20 mph across, and the resulting wind vector of 72.8 mph. The 'ceiling' of the wind tunnel is depicted by the blue rectangle just inside the edges of the figure. The 16.8-degree rotation of the model is also depicted.

As shown in Figure 3.7, the chosen wind speeds were 70 mph (112.6 km h) head on, being the average of the speeds in the previous scenario, with a 20 mph (32.2 km h) crosswind. 20 mph was chosen because it is strong enough to be significant, but not a crazy gale-force wind where one might choose to avoid riding a motorcycle all together.

The resulting flow had a wind speed of 72.8 mph (117.2 km h) incident on the model at 16.8 degrees off normal. Intuitively, if a motorcycle were moving forward at freeway speeds while experiencing a horizontal crosswind, the motorcycle will overall observe, in its frame of reference, wind approaching it diagonally. To simulate this in the CFD setup, I rotated the models about their vertical axis within the wind tunnel by 16.8 degrees, then set the parameters of the tunnel itself to produce a 72.8 mph flow. Luckily, the axes Autodesk CFD uses to calculate force vectors are locked to the orientation of the motorcycle, so I could easily collect the Y and Z direction force magnitudes and locations relative to the motorcycle, not relative to the tunnel. In other words, the measured horizontal force was the force being applied exactly normal to the side of the motorcycle, rather than 16.8 degrees off normal.

There were a few other parameters set during all simulations which can be briefly summarized. Air was supposed at sea level and room temperature[14] and simulated as an incompressible (discussed in CFD section) fluid. Each simulation was run for 100 steps which was more than enough to fully develop and stabilize the flow. The mesh sizing was set slightly fine at 0.75, with 1 being the program's default setting (lower numbers mean increased fineness mean smaller cells) to increase accuracy[15]. I used Autodesk CFD's auto mesh sizing and adaptive mesh sizing, which increased the fineness of the mesh around the motorcycle and specifically on sharper angles/curves while reducing the mesh sizing away from the motorcycle (on the edges of the volume) and on flat sections to increase accuracy without sacrificing performance. All model surfaces were assigned as rigid bodies made of aluminum (material did not affect the

[14] 21 Celsius, 70 Fahrenheit.
[15] Return to Figure 2.1 for a representation of a 0.75 mesh

behavior in this setup). Finally, the total number of cells in the simulations, as described, ranged for 9-12 million, depending on the model.

In the CFD simulation setup, there was one significant simplification made which will impact the accuracy of the results: the wheels were simulated as being stationary. During a freeway cruising at around 70 mph, the average wheel will be spinning at about 1000rpm. This will affect the airflow around the motorcycle in two ways. First, the spinning spokes of the wheels will create turbulent air which will impact the laminar flow around the sides of the motorcycle. Second, the rotating tire will have lower aerodynamic drag below its centerline, and higher aerodynamic drag above the centerline because the top will be rotating into the wind, while the bottom rotates away from it. This will cause the top to cast a slightly larger wake than the bottom. It is not uncommon to simulate wheels as being stationary during CFD testing even at the professional level [3] since the effects are measurable but not pronounced and can be difficult to accurately model.[9] This simplification, like most throughout this project, was made to decrease complexity and computation time. Including rotating wheels would be a useful next step for future research into the potential for a rear fairing design.

With the properties and simplifications in both the CAD Models and CFD setup outlined, it time to discuss the data collection process and results. Spoiler alert, it works!

Results

The data collection process can be broken down into three phases.

In the first phase I checked whether the behavior of the models and CFD simulations was consistent with predictions. In this phase NF1 was used to establish a baseline and the relationship between force of drag and airspeed was compared with predictions. The flow around the motorcycle was also compared with predictions. Then, the performance of F1 was compared to NF1 to establish that the fairing design was working as expected.

The second phase was designed to determine the relationship between the improvements in drag coefficient with the addition of the rear fairing and the 'starting' drag coefficient of the front fairing. The front fairing was redesigned to NF2 which had a lower drag coefficient than NF1, and N2F1was created by adding the first rear fairing design to the NF2 model. The performance improvements from NF1 to F1 were then compared to the improvements from NF2 to N2F1 to determine whether the drag coefficient of the front fairing affected the performance of the rear fairing.

Phase three of testing involved trying to achieve the best performance, both in head-on and crosswind scenarios, of the rear fairing design. After redesigning the rear fairing to create F2 based on the lessons learned in F1, three variations on the F2 design were created to test how the length and porousness of the fairing affected its performance. At this stage all relevant models were tested both in the head-on and crosswind scenarios.

During the head-on testing at four freeway speeds, the force magnitudes, and locations in the X direction (force of drag) and the Y- direction (force of lift), were

collected. During the crosswind scenarios force magnitudes and locations in the X, Y and Z directions were collected.

All numerical data gathered during this process was rounded to five significant figures after initial collection and during the processing phase. Data processing (to calculate drag coefficient and predicted range) and graph making was done using python. Images were captured within Autodesk CFD, some were edited and enhanced for clarity.

Phase One: Establishing Consistency

The first test conducted in phase 1 was the head-on scenario at four different freeway speeds for the NF1 model. The results are shown in Table 1.

SPEED (MPH)	FORCE (N)	Calculated Cd	Average Cd	Std. Dev. of Average Cd	Range Est. (km)
55	206.18	0.80111	0.80363	0.00342	122.5
65	288.24	0.80187			
75	387.00	0.80865			
85	493.53	0.80287			

Table 1: NF1 Results

All subsequent tables with the same format were calculated using the same methods. Cd was calculated using Equation 2 (Figure E.2). These were then averaged, and their standard deviation calculated. The range was estimated using Equation 1 (Figure E.1), with the measured frontal area and average drag coefficient.

Each drag coefficient value was calculated by inputting the speed and force-of-drag values into equation 2. Equation 2 assumes a squared relationship between the force-of-drag and the speed of oncoming air. That the resultant drag coefficients across the measured range of speeds have a standard deviation of .0034 against an average of .80 is indicative of a strong adherence to that relationship. The drag coefficients should not

to change significantly from one speed to the next. The consistency in drag coefficient demonstrates that the CFD simulations are, by this metric, modeling the system realistically enough to reflect the expected relationship between speed and force of drag. This adherence was maintained, as demonstrated by subsequent results, throughout the entire testing process.

The measured average drag coefficient for the NF1 model is high in the spectrum of expected drag coefficient measurements. As discussed in the introduction and first section, a drag coefficient in the 0.40 - 0.55 range is indicative of a fairinged motorcycle, while drag coefficients in the 0.55 - 0.90 range are indicative of ‘naked’ style designs. Based on our discussion of aerodynamics, and the simplifications made in this model, there are two significant factors which could be contributing to this elevated measured value.

The first is the elimination of paths for air to travel through the front fairing, like those that would be used for cooling. Instead of having open holes through the center of the bike, this design simplifies this area to a slightly concave wall--the least aerodynamically efficient shape. The second is the size of the rider. This model was created based on measurements of myself, but I am of above average height and shoulder width. It’s impossible to know what size of person was used when measuring drag coefficients for other bikes, but the size of rider will significantly affect the aerodynamic performance. A tall, broad torso will exacerbate the problems of low-pressure area being created behind the rider, and I suspect this contributed to the overall high measured drag coefficient.

Additionally, the large size of rider contributed to a calculated frontal area of $0.6945m^2$. This was high on the spectrum of motorcycle frontal areas and thus resulted in a lower estimated range across all models.

The second set of measurements taken in phase one used F1, results of which are shown in Table 2.

SPEED (MPH)	FORCE (N)	Calculated Cd	Average Cd	Std. Dev. of Average Cd	Range Est. (km)
55	194.02	0.75387	0.75770	0.00304	128.4
65	272.07	0.75688			
75	363.30	0.75912			
85	467.73	0.76090			

Table 2: F1 Results

Again, there was a low standard deviation, meaning a high consistency with predicted relationships. Compared to NF1, the addition of the rear fairing reduced the drag coefficient by 0.040, which resulted in a modest increase in estimated range of 6 km (3.7 miles).

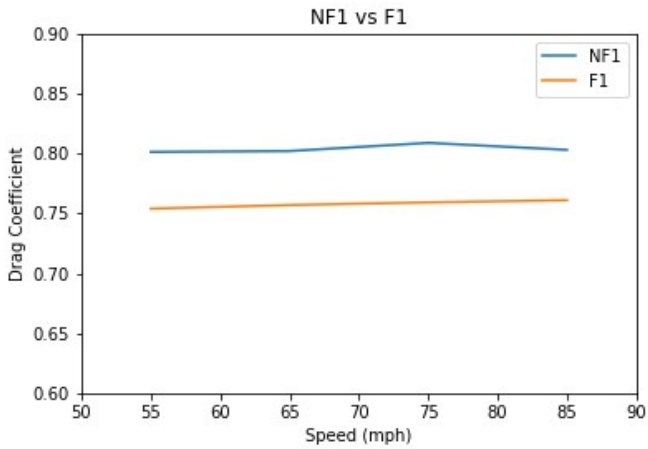

Figure 4.1: Graph NF1 vs F1

This graph compares the measured Cd values of NF1 and F1. Each line is made by connecting the four measure data points. Both axes have a relative scale.

Figure 4.1 shows a graph comparing the Cds of F1 and NF1. While both demonstrate a high level of consistency across all speeds, at this scale there is evidence of a slight upward trend, where drag coefficient increases with speed. This behavior is likely a result of higher speeds causing the motorcycle to cast a longer wake and thus increasing the volume of low-pressure air behind the bike.

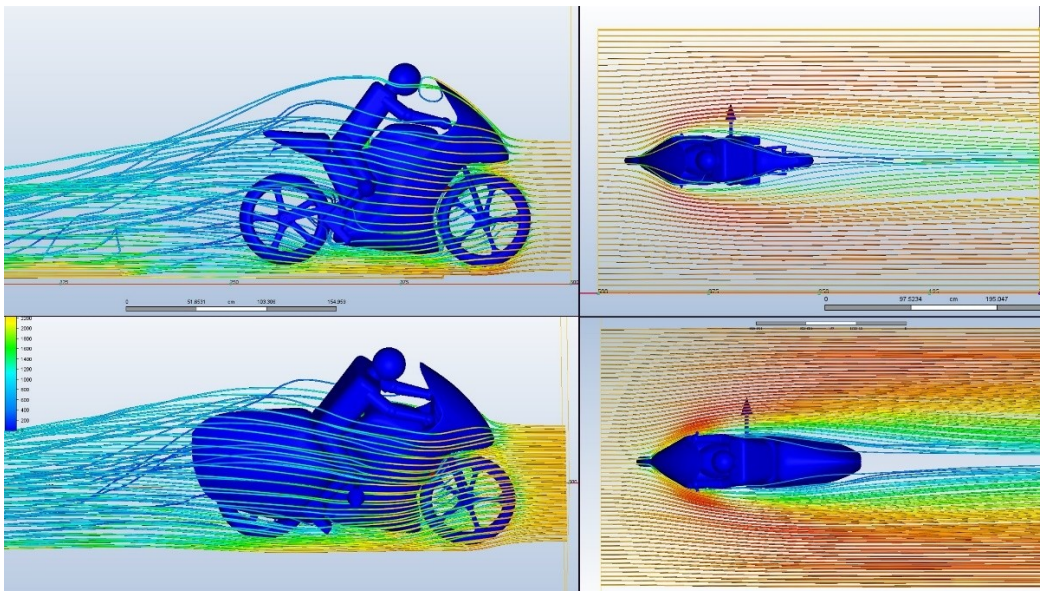

Figure 4.2: Flow Around NF1 vs F1

All four images depict flows measured at an airspeed of 55 mph. The top two are from model NF1, the bottom, F1.

Figure 4.2 shows a comparison of the flow around NF1 and F1 and reveals that the rear fairing is, for the most part, working as predicted. The left images show that in the area just behind the rider on the lower section of the bike, F1 exhibits brighter, parallel lines characteristic of laminar flow and there is an overall reduction in the turbulence behind the motorcycle compared to NF1. This was exactly the performance improvement expected.

Further examination of the flow around F1, using the second left set of images, revealed the tail section was tucking (reducing in width) too quickly, and the laminar flow was breaking away from rear fairing before the end, shown by the lines transitioning to dark blue right at the tail of the model, reducing its performance. Also observed in this flow comparison was that the leading edge of the front fairing, right around the ‘air intake’ was too steeply raked and was causing the air to be accelerated

out away from the edges of the bike before it even reached the rider's legs (casting a wake around the rest of the motorcycle). Force was being unnecessarily applied to moving the air horizontally, increasing the drag coefficient of the front fairing. These observations motivated the redesign of both the front and rear fairing.

The redesign of the front fairing to NF2 also presented an opportunity to gain insight into the relationship between the drag coefficient of the front fairing and the improvement as a result of the rear fairing.

Phase Two: Relationship Between Front Fairing Cd and Rear Fairing Performance

During phase one of testing the rear fairing was demonstrated to reduce drag coefficient by 0.040, which, at the measured drag coefficient of 0.80, represented a 5.7% improvement and only resulted in a 6km increase in range. This observed drag coefficient was high compared to expectations. Because range is related to drag coefficient by a $1/r^2$ relationship (see Equation 1, Figure E.1), a similar improvement starting from a motorcycle design with a lower drag coefficient will result in a greater increase in range. The objective of phase two was to establish whether the improvement in drag coefficient is dependent on the drag coefficient of the front fairing, in pursuit of understanding how these measurements might translate to an improvement on a motorcycle with more realistic (lower) starting drag coefficient.

If the improvement is dependent on the drag coefficient, for example, adding the rear fairing will always result in a 5% improvement. From a starting drag coefficient of 0.40, the rear fairing would reduce the Cd to 0.38 and add 7km of range. However, if the improvement is independent of drag coefficient, meaning adding the rear fairing

will always reduce the drag coefficient by 0.040 regardless of the starting point, then 0.40 would become 0.36 with the addition of the rear fairing, and the vehicle would gain 15km of range.

To test this, I redesigned the front fairing to be more aerodynamically efficient by addressing the problems observed in the first section, without changing its overall size or shape, creating NF2. I then added the first iteration of the rear fairing design to the NF2 model, yielding N2F1. The results of the NF2 and N2F1 tests can be found in Tables A.1 and A.2 in the Appendix but their measured drag coefficients were NF2: 0.78393 ± 0.00533 and N2F1: 0.74144 ± 0.00433. I created Table 3 and Figure 4.3, comparing the change in drag coefficient from NF1 to F1, and NF2 to N2F1.

SPEED (MPH)	NF1 - F1	Average Difference	NF2 - N2F1	Average Difference
55	0.04724	0.0459 ± 0.0065	0.04459	0.0425 ± 0.0097
65	0.04499		0.04060	
75	0.04953		0.03918	
85	0.04197		0.04562	

Table 3: Performance Comparison of NF1-F1 and NF2-N2F1

Columns 2 and 4 were made by subtracting the drag coefficients at each speed. Columns 3 and 5 represent the averages of columns 2 and 4 respectively. The errors are sums of standard deviations of the source averages, i.e. Column 3 = (Std. Dev. Avg. Cd F1) + (Std. Dev. Avg. Cd NF1).

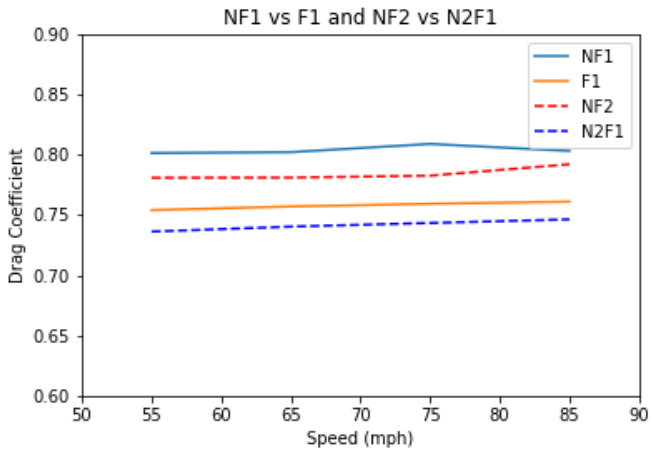

Figure 4.3: Graph Comparing NF1, F1, NF2 and N2F1

Unfortunately, this data is largely inconclusive. The problem being the redesign from NF1 to NF2 only yielded an improvement in average drag coefficient of 0.02. Coupled with the fact that it was prohibitively time consuming to redesign the front fairing again to further improve its drag coefficient *without changing its size and thus frontal area*, this very minor improvement means the two data points with which I might try and extrapolate a relationship (already an insufficient number to prove anything other than linear interaction) are very close together in the grand scheme of possible drag coefficients. This closeness makes distinguishing between the dependent and independent hypotheses dependent on extreme accuracy. The dependent hypothesis predicts the Cd of N2F1, will be 94.3% of NF2, or 0.7391 (equating to an improvement of .04483), while the independent hypothesis predicts the Cd of N2F1 be 0.0459 less than NF2, or 0.7386. While the standard deviations in the calculated average drag coefficients are relatively small compared to the drag coefficients themselves, when considering the difference between drag coefficients, these standard deviations add together as error. Since these differences are on the order of 0.04, the summed standard

deviations become significant errors. The range of possible values for NF1 - F1 is contained entirely within the range of NF2 - N2F1. The range for NF2 - N2F1 also contains the values for the difference predicted by both hypotheses.

The only thing that can be said about the data is that the average value of the difference NF2 - N2F1, and the average value of the Cd for N2F1, are *closer* to the dependent prediction than the independent prediction.

So, the data collected in phase two was not conclusive enough to establish a clear relationship between the drag coefficient of the front fairing and the performance of the rear fairing. Regardless, I could still try to improve the performance of my rear fairing and test the effects of two properties on the rear fairing's ability to reduce Cd and stability in crosswind scenarios.

Phase Three: Cross Wind Scenarios and Porous Fairings

The first test in phase three was of the redesigned (based on the observations from phase one) rear fairing, model F2. Results from this test are shown in Table 4. The second version of the rear fairing resulted in a further 0.0166 improvement in drag coefficient over the N2F1 design, making the overall improvement as a result of the rear fairing (NF2-F2) 0.05912, or 7.54%, with an increase in range of 8 km (5 miles).

SPEED (MPH)	FORCE (N)	Calculated Cd	Average Cd	Std. Dev. of Average Cd	Range Est. (km)
55	185.42	0.72043	0.72481	0.00346	133.0
65	260.21	0.72388			
75	347.66	0.72646			
85	447.78	0.72845			

Table 4: F2 Results

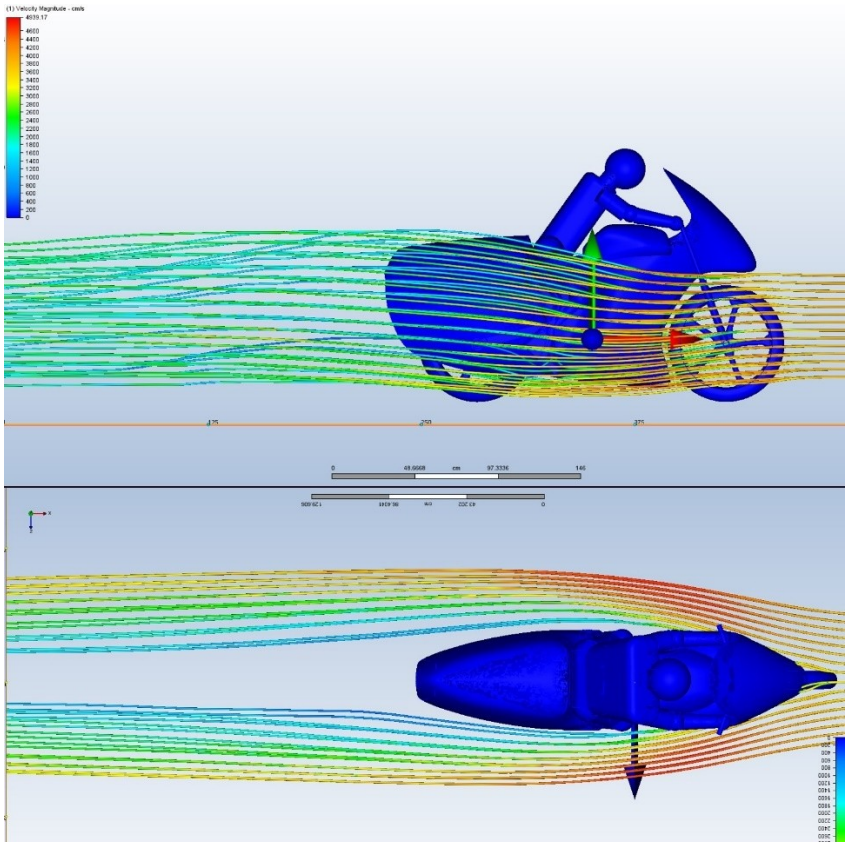

Figure 4.4: Flow Around F2

Both Images depict 85 mph flow over the F2 model.

Images of the flow around F2 can be seen in Figure 4.4. Observe how the air's path is consistent along the entire length of the motorcycle, inducing over the rear section, with clear parallel lines that do not devolve into turbulence. Additionally, the effects of the redesigned front fairing can be seen with a reduction in the overall intensity of the wake being cast by the leading edge of the fairing. The wake also parts from the bike at a shallower angle.

With the design of rear fairing now more effective, and anticipating the crosswind scenario testing, I developed three more variations on the concept. These

variations were designed to test the effects of two different methods for reducing the horizontal surface area of the design without increasing drag coefficient: shortening the overall length of the fairing and adding vertically cut holes. Thus, were formed models SF, FH and SFH. Tables A.3, A.4 and A.5, showing the results of the head-on freeway-speed scenario for all three new models, can be found in the Appendix. Figure 4.5 shows a graph of their performance, alongside F2 and NF2.

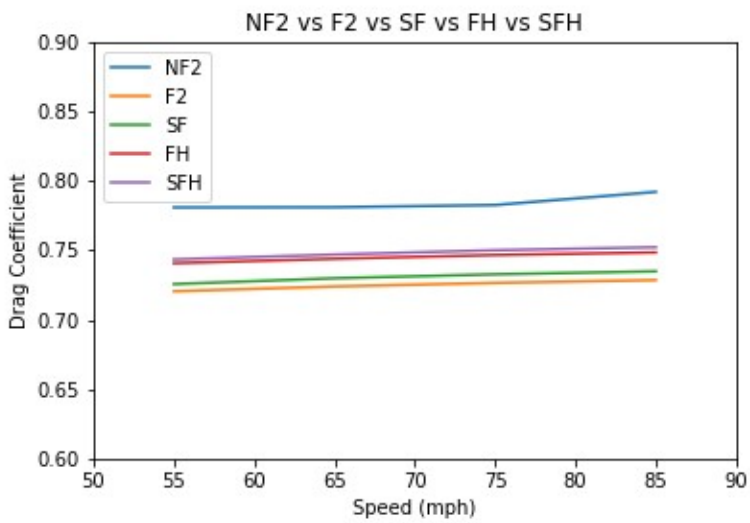

Figure 4.5: Comparison Graph of the Measured Drag Coefficients of NF2, F2, SF, FH and SFH

Shorting the rear fairing by 5 inches had a very minimal effect on its performance, increasing the drag coefficient by only 0.0059. Adding the holes had a slightly more significant effect on the performance of both F2 and SF, increasing their Cds by about 0.018. This means the ‘holed’ fairings reduced the drag coefficient by 30% less than their non-holed counterparts, thus performed 3% worse in overall system drag coefficient and had 2.1% lower range estimates.

To determine whether these losses in performance would translate to increased (or less decreased) stability, I had to test all five models (NF2, F2, SF, FH, SFH) in the

crosswind scenario. Using the simulation setup described in the methods section I collected data on the horizontal (Y direction) force's magnitude and location, and on the lift force's (Z direction) magnitude and location. Unfortunately, the origin for the axes, which was locked to the geometry of each model, was different across each model as it was determined by Autodesk CFD's estimation of the center of mass (which was completely wrong, because none of the internals of the bike were modeled). This means that the comparison of the locations of the centers of force had to be done visually.

Models	Force Y direction	Diff. from NF2	Force Z direction	Diff. From NF2
NF2	367.56	+ 0%	10.99	- 0%
F2	450.82	+ 22.7%	3.60	- 67.2%
SF	453.30	+ 23.3%	5.10	- 53.6%
FH	447.02	+ 21.7%	3.57	- 67.5%
SFH	443.56	+ 20.7%	1.08	- 90.2%

Table 5: Crosswind Test Results Comparison for NF2, F2, SF, FH and SFH

Columns two and four show the measured force magnitudes. Columns three and five compare these measured values (as percentages above or below 100) to those of NF2. Force in Y direction is the horizontal force, force in direction is the force of lift.

Table 5 shows the measured magnitude of horizontal and lift forces in each test and includes a comparison between the measured values of the rear-fairing bikes and NF2. As expected, all four rear fairing designs increase the total horizontal force on the bike, although only by 21-23%. However, they all decrease the force of lift by between 50 and 90%.

Worthy of note is that this same decrease in lift was present in the freeway speeds-testing, and in all cases it was accompanied by a shifting of the center of lift rearward, resulting in a tendency for the motorcycle to put more weight on its front, increasing rider control. Also noteworthy is that, while the SFH model performs slightly

better than the FH model in both horizontal and vertical force metrics, the SF model is actually the worst performing, even worse than the longer F2 model. The SFH model was the best performing in this test, but the worst performing in the Cd comparison.

As discussed in the motorcycle stability section, the magnitude of these forces does not tell the whole story. Since numerical comparison was impossible, Figure 4.6 shows a visual comparison (edit for clarity) of the locations of the centers of force in the horizontal direction for NF2 and F2 (marked by the green dot). It also includes white circles representing estimates for the centers of mass of the motorcycles. These estimates are based on a slightly forward biased weight distribution, as is common in motorcycles, and low center of gravity common on electric motorcycles. The center of force in the horizontal direction was similarly placed for all rear-fairing bikes, moving only slightly (less than 1 cm) forward for the shorter versions.

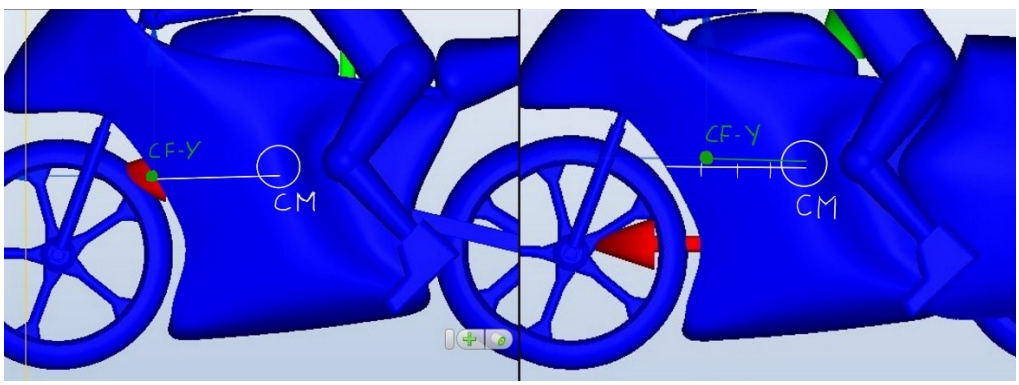

Figure 4.6: Comparison of the Center of Horizontal Force Between NF2 and F2

The green dot was placed over a harder-to-see red dot calculated within the CFD program and represents the center of force applied in the Y-direction. White circles represent estimates for center of mass.

The white line on the F2 (right) side is subdivided by 3 even spaced vertical lines. Compared to the center of y-directional force on NF2, the center on F2 is moved a

little more than 25% closer to the estimated center of mass and is only slightly higher off the ground. Based on the toque analysis techniques developed in the stability section, this means, in a crosswind scenario, model F2 will experience about 23% more torque trying to roll it to the side (f increases by 23%, *r* stays about the same) but a 7.25% decrease in torque trying to rotate it out of the wind (123% of the force, 75% radius -> 92.25% torque) when compared with NF2. This analysis will be similar for the other three rear fairing designs.

Discussion of Results

Comparing the performance of F2, across all metrics, with that of NF2, the addition of the rear fairing will result in: a 6.4 % increase in freeway cruising range, a 50% reduction in aerodynamic lift, an increased tendency to roll onto the front wheel generating more grip and improving rider control and a 7.5% reduction in yaw-torque, but a 23% increase in roll-torque, when experiencing a crosswind.

A motorcycle with this rear fairing design will go a little bit farther, and, in the absence of a significant crosswind, will feel more stable (lower lift, increased rider control). In the presence of a strong crosswind, this lower lift will remain and the nose will feel less like it wants to be turned away from the wind, but the rear-fairinged motorcycle will be noticeably more likely to roll over.

Shortening the fairing and/or adding holes will diminish the range by about 2.1%, but further reduce the lift, and decrease the rollover toque by 1.9%. In other words, a holed, or shortened and holed, rear-fairinged motorcycle will go slightly less distance, but be a little more stable compared to the unmodified design.

However, these results are not complete. The drag coefficients measured on the NF1 and NF2 models were significantly above expectations, making improvements in drag coefficient have a lower effect on range. The inconclusiveness of the tests to establish a relationship between front fairing drag coefficient and rear fairing performance make it impossible to accurately extrapolate the improvements measured here to motorcycles with a lower drag coefficient (where the addition of the rear fairing would have a greater effect on range). Also, the parameters of the CFD setup were, in some cases, chosen to be less accurate in favor of reduced computation time. Finally, the design of the holes was arguably arbitrary, but an entire second round of research and experimentation could be dedicated just to devising the best hole-design to reduce horizontal force without increasing drag coefficient.

Conclusion

Electric vehicles present a promising path towards large-scale, fast, and flexible long-distance travel powered by renewable resources. Motivating their adoption requires improving their performance to match or exceed that of conventional, gas powered vehicles. For electric motorcycles, this means increasing cruising range without adding weight, which is achievable through amelioration of aerodynamic efficiency. The rear fairing design created and tested for this thesis has demonstrated potential to increase aerodynamic efficiency and motorcycle stability in some metrics, but also heighten susceptibility to crosswind scenarios. The designs and testing methods used to attain these results represent a rigorous, but far from exhaustive, investigation. There is still a lot of development work to be done.

Future research of this design would involve continued experimentation with variations of the basic shape and attempt to increase its drag reduction capabilities while lowering crosswind susceptibility. Promising avenues include a detailed investigation of possible hole designs, and fine testing of length parameters to determine the optimum fairing size. More realistic CAD models and simulation setups, capable of closely matching real-world drag coefficients for the starting front fairing design, would enable a more accurate understanding of the potential for performance enhancements through the addition of a rear fairing.

Aerodynamic development of a new design can take years and teams of full-time engineers to achieve. This thesis represents the first cursory check of an idea. Based on the results of this check, my rear-fairing idea is sound, making it worthy of further investigation. As a means to notably increase efficiency and performance, in a

market as competitive, fast growing and environmentally relevant as the electric transportation industry, “worthy of further investigation” is a good place to be. I definitely plan on pursuing development. The motorcycle enthusiast in me is giddy at the idea of throwing a leg over a cyberpunk-styled, electric, rear-fairinged, high speed performance motorcycle and cruising my hometown freeways for miles on end.

Appendix: Additional Figures and Tables

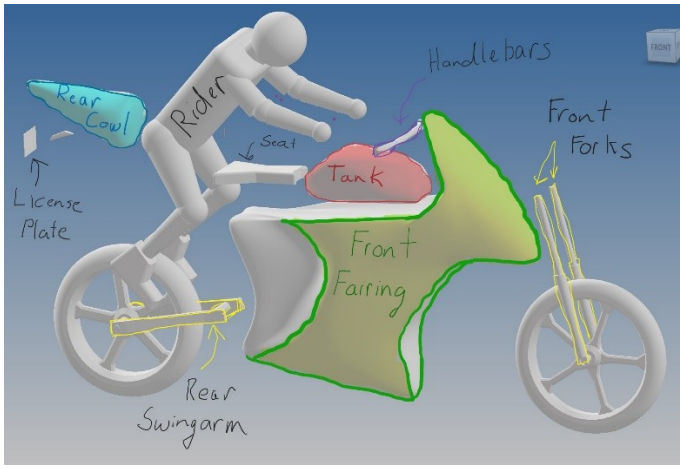

Figure A.1: The Anatomy of a Motorcycle

$$E = 11.3488kWh$$

$$m = 208kg$$

$$f = 0.04$$

$$v = 112.7km/h$$

$$\rho = 1.2754kg/m^2$$

Figure A.2: Values Used in the Range Estimation Equation

These were collected from [19] or based on chosen parameters

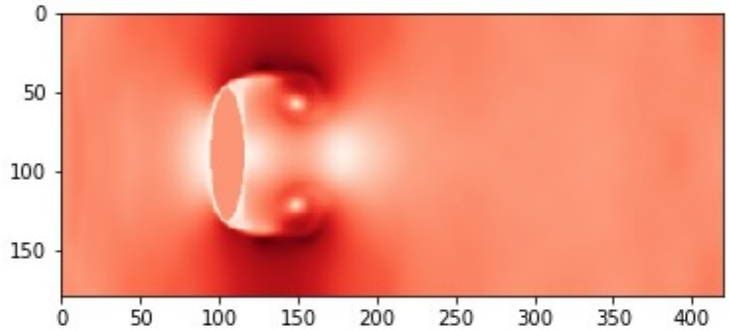

Figure A.3: Vortex Formation Around the Edge of an Object in a 2-dimensional CFD Simulation.

In this image, the flow moves from left to right. The darkness of the red increases with flow speed. This image was created using python for a simulation class.

SPEED (MPH)	FORCE (N)	Calculated Cd	Average Cd	Std. Dev. of Average Cd	Range Est. (km)
55	200.92	0.78068	0.78393	0.00533	125.0
65	280.67	0.78081			
75	374.44	0.78240			
85	486.74	0.79183			

Table A.1: NF2 Results

SPEED (MPH)	FORCE (N)	Calculated Cd	Average Cd	Std. Dev. of Average Cd	Range Est. (km)
55	189.44	0.73609	0.74144	0.00433	130.6
65	266.08	0.74021			
75	355.69	0.74322			
85	458.70	0.74621			

Table A.1: N2F1 Results

SPEED (MPH)	FORCE (N)	Calculated Cd	Average Cd	Std. Dev. of Average Cd	Range Est. (km)
55	186.75	0.72560	0.73069	0.00396	132.1
65	262.33	0.72979			
75	350.61	0.73261			
85	451.66	0.73477			

Table A.3: SF Results

SPEED (MPH)	FORCE (N)	Calculated Cd	Average Cd	Std. Dev. of Average Cd	Range Est. (km)
55	190.6	0.74058	0.74479	0.00338	130.2
65	267.36	0.74377			
75	357.24	0.74648			
85	460.01	0.74834			

Table A.4: FH Results

SPEED (MPH)	FORCE (N)	Calculated Cd	Average Cd	Std. Dev. of Average Cd	Range Est. (km)
55	191.31	0.74334	0.74803	0.00381	129.7
65	268.45	0.74680			
75	358.89	0.74992			
85	462.30	0.75721			

Table A.5: SFH Results

Bibliography

[1] Angeletti, Mario, Lucia Sclafani, Gino Bella, and Stefano Ubertini. "The Role of CFD on the Aerodynamic Investigation of Motorcycles." *SAE Technical Paper Series* 112 (March 2003): 1103–11. https://doi.org/10.4271/2003-01-0997.

[2] "Aerodynamics." *Aerodynamics - New World Encyclopedia*, New World Encyclopedia, www.newworldencyclopedia.org/entry/Aerodynamics.

[3] Axon, Lee, Kevin Garry, and Jeff Howell. "An Evaluation of CFD for Modelling the Flow Around Stationary and Rotating Isolated Wheels." *SAE Technical Paper Series* 107 (January 1998): 205–15. https://doi.org/10.4271/980032.

[4] Blocken, Bert. "Computational Fluid Dynamics for Urban Physics: Importance, Scales, Possibilities, Limitations and Ten Tips and Tricks towards Accurate and Reliable Simulations." *Building and Environment* 91 (February 25, 2015): 219–45. https://doi.org/10.1016/j.buildenv.2015.02.015.

[5] "Carbon Pollution from Transportation." *EPA*, Environmental Protection Agency, (June 10, 2019): www.epa.gov/transportation-air-pollution-and-climate-change/carbon-pollution-transportation.

[6] Cauwer, Cedric De, Joeri Van Mierlo, and Thierry Coosemans. "Energy Consumption Prediction for Electric Vehicles Based on Real-World Data." *Energies* 8, no. 8 (December 2015): 8573–93. https://doi.org/10.3390/en8088573.

[7] Cossalter, Vittore. *Motorcycle Dynamics*. 2nd ed., n.d. ISNB 978-1-4303-0861-4

[8] Foale, Tony. "Aerodynamics." Moto Chassis (1997). https://motochassis.com/Articles/Aerodynamics/AERO.htm.

[9] Hobeika, T., and S. Sebben. "CFD Investigation on Wheel Rotation Modeling." *Journal of Wind Engineering and Industrial Aerodynamics* 174 (2018): 241–51. https://doi.org/10.1016/j.jweia.2018.01.005.

[10] Keogh, J., et al. "Flow Compressibility Effects around an Open-Wheel Racing Car." *Aeronautical Journal*, vol. 118, no. 1210, (Dec. 2014): 1409–1431.

[11] Keogh, James, et al. "The Influence of Compressibility Effects In Correlation Issues for Aerodynamic Development of Racing Cars." *18th Australasian Fluid Mechanics Conferense*, (Dec. 7, 2012).

[12] Sarrafan, Kaveh, Danny Sutanto, Kashem M. Muttaqi, and Graham Town. "Accurate Range Estimation for an Electric Vehicle Including Changing Environmental Conditions and Traction System Efficiency." *IET Electrical*

Systems in Transportation 7, no. 2 (January 2017): 117–24. https://doi.org/10.1049/iet-est.2015.0052.

[13] Sharma, A., and D. J. N. Limbeer. "Design of a Novel Aerodynamically Efficient Motorcycle." *Bicycle and Motorcycle Dynamics*, October 20, 2010.

[14] Sripathi, Venkata Aditya. "The Impact of Active Aerodynamics on Motorcycles Using Computational Fluid Dynamics Simulations." *All Theses, Dissertations, and Other Capstone Projects* 721 (May 2017).

[15] Uhlarik, Michael. "Motorcycle Aerodynamics." Canadas Moto Guide, May 4, 2016. https://canadamotoguide.com/2016/05/04/motorcycle-aerodynamics/.

[16] "U.S. Energy Information Administration - EIA - Independent Statistics and Analysis." *Use of Energy for Transportation - U.S. Energy Information Administration (EIA)*, www.eia.gov/energyexplained/use-of-energy/transportation.php.

[17] Weir, David H., and John W. Zellner. "Lateral-Directional Motorcycle Dynamics and Rider Control." *SAE Technical Paper Series*, January 1978, 1364–88. https://doi.org/10.4271/780304.

[18] Wolfram, Stephen. *A New Kind of Science*. Wolfram Media, 2002, 996.

[19] Zero Motorcycles, 2017 Zero Sr, https://www.zeromotorcycles.com/zero-s/2017/specs.php